

Rare transmission of commensal and pathogenic bacteria in the gut microbiome of hospitalized adults

Benjamin A. Siranosian¹, Erin Brooks², Tessa Andermann³, Andrew R. Rezvani⁴, Niaz Banaei^{5,6,7}, Hua Tang¹, Ami S. Bhatt^{*1,2,4}

1. Department of Genetics, Stanford University, Stanford, CA, USA
2. Department of Medicine, Division of Hematology, Stanford University, Stanford, CA, USA.
3. Division of Infectious Diseases, University of North Carolina at Chapel Hill, Chapel Hill, North Carolina
4. Department of Medicine, Division of Blood and Marrow Transplantation and Cellular Therapy, Stanford University School of Medicine, Stanford, CA
5. Department of Medicine, Division of Infectious Diseases and Geographic Medicine, Stanford University, Stanford, CA, USA.
6. Clinical Microbiology Laboratory, Stanford University Medical Center, Stanford, CA, USA
7. Department of Pathology, Stanford University, Stanford, CA, USA.

* to whom correspondence should be addressed: asbhatt@stanford.edu

Abstract

Bacterial bloodstream infections are a major cause of morbidity and mortality among patients undergoing hematopoietic cell transplantation (HCT). Although previous research has demonstrated that pathogenic organisms may translocate from the gut microbiome into the bloodstream to cause infections, the mechanisms by which HCT patients acquire pathogens in their microbiome have not yet been described. We hypothesized that patient-patient transmission may be responsible for pathogens colonizing the microbiome of HCT patients, and that patients who share time and space in the hospital are more likely to share bacterial strains.

Here, we used linked-read and short-read metagenomic sequencing to analyze 401 stool samples collected from 149 adults undergoing HCT and hospitalized in the same unit over five years. We used metagenomic assembly and strain-specific comparison methods to investigate transmission of gut microbiota between individuals. While transmission of pathogens was found to be rare, we did observe four pairs of patients who harbor identical or nearly identical *E. faecium* strains in their microbiome. These strains may be the result of transmission between patients who shared a room and bathroom, acquisition from a common source in the hospital or transmission from an unsampled source.

We also observed identical *Akkermansia muciniphila* and *Hungatella hathewayi* strains in two pairs of patients. In both cases, the patients were roommates for at least one day, the strain was absent in the putative recipient's microbiome prior to the period of roommate overlap and the putative recipient had a microbiome perturbed by antibiotic treatment for a bloodstream infection. Finally, we identified multiple patients who acquired identical strains of several species commonly found in commercial probiotics and dairy products, including *Lactobacillus rhamnosus*, *Lactobacillus gasseri* and *Streptococcus thermophilus*. Overall, the limited amount of putative transmission observed indicates that current infection control and contact precautions are successful in preventing interpersonal exchange of microbes. However, the potential transmission of commensal microbes with immunomodulatory properties raises questions about the recovery of microbiome diversity after HCT, and indicates that patients in this setting may acquire new microbes by sharing space with others.

Introduction

Patients undergoing hematopoietic cell transplantation (HCT), a potentially curative treatment for a range of hematologic malignancies and disorders, are at increased risk for bloodstream infections (BSIs) and associated morbidity and mortality¹. While the bacterial pathogens that cause BSIs in HCT patients are well understood, their routes of transmission are often unclear. Determining these transmission pathways involves identifying two critical elements: the source of the infection, i.e., how the pathogen was introduced into the patient's bloodstream, and the origins of the particular pathogen causing the BSI.

The most common ways bacterial pathogens can be introduced into an HCT patient's bloodstream include contaminated central intravenous lines and translocation of intestinal microbiota across a damaged epithelium². Indeed, research from our group and others has shown that strains of bacteria isolated from the blood of HCT patients with BSIs may be indistinguishable from the strains in the intestinal microbiota of these patients prior to infection³⁻⁵. In addition, HCT patients with a microbiome dominated by a single bacterial taxon, such as *Enterococcus* or *Streptococcus*, are at increased risk for not only BSI^{6,7}, but also graft-versus-host disease^{8,9} and death¹⁰⁻¹³.

Identifying the source of the BSI is only the first step. To fully understand the transmission pathways of bacterial pathogens in hospital settings, it is also essential to determine the origin of the pathogen that caused the BSI. For gut-based pathogens, there are three possibilities. First, they may exist in the HCT patient's microbiome upon admission to the hospital. Second, hospital environments and equipment may serve as unintentional reservoirs of pathogens, thereby infecting multiple patients through exposure¹⁴. Lastly, a pathogen could originate from the microbiome of another patient and be transmitted via shared spaces. In cases where traditional epidemiological links cannot be found, this patient-patient transmission of gut microbes may be the "missing link" that explains the persistence of BSIs in hospital environments¹⁵.

Transmission of gut bacteria and phages between individuals is known to occur in specific cases, such as from mothers to developing infants¹⁶⁻¹⁸. By contrast, adults have a microbiome that is relatively

resistant to colonization with new organisms even after perturbation by antibiotics^{19–21}. While adults living in the same household or in close-knit communities may have more similar microbes than those outside the group²², to our knowledge, direct transmission of gut microbes between adults has not been observed with high-resolution metagenomic methods. Transmission of gut microbiota is thought to occur by a fecal-oral route, which could happen in the hospital environment by exposure to contaminated surfaces or equipment, sharing a room or bathroom, contaminated hands of healthcare workers or other sources. The perturbed microbiomes of HCT patients, often lacking key species to provide colonization resistance, may be primed to acquire new species from these sources.

Previous studies of the microbiome in HCT patients have often used 16S rRNA sequencing^{10,23–25}, which is sufficient for taxonomic classification but cannot differentiate specific strains in a mixed community. By contrast, short-read shotgun metagenomic sequencing can capture information from all bacterial, archaeal, eukaryotic and phage DNA in a stool sample. While short-read sequencing data is accurate on a per-base level, it is often insufficient to assemble complete bacterial genomes due to the presence of repetitive genetic elements. Linked-read sequencing captures additional long-range information by introducing molecular barcodes in the library preparation step. This technology allows for significant increases in assembly contiguity^{26,27} while retaining high per-base accuracy. Both of these technologies also capture information about strain diversity, genetic variation within the population of a species^{28,29}, which is critical for measuring transmission between microbiomes.

Here, we use a collection of short-read and linked-read metagenomic sequencing datasets from 401 stool samples to analyze bacterial transmission between HCT patient microbiomes at a single, high volume hospital. We apply strain-resolved comparison methods to show that transmission of bacteria between adults hospitalized in the same unit at the same time is likely a rare event, usually occurring when recipients have extremely perturbed microbiomes, such as after exposure to broad-spectrum antibiotics. Bacterial strains shared between individuals include both pathogenic and commensal organisms, demonstrating that transmission may depend more on niche availability than pathogenicity or antibiotic resistance capacity. We find that pathogens colonizing HCT patient microbiomes are present in

the first sample in a time course roughly 60-70% of the time in our cohort. This suggests that in most cases, prior colonization, rather than direct transmission from other patients or the hospital environment, is responsible for pathogenic organisms in the gut microbiomes of this patient population. Despite the fact that patients were frequently placed into double occupancy hospital rooms with a shared bathroom, we observe relatively few putative transmission events. This implies that current infection control procedures are working as intended, and that sharing a room with another patient may not place a patient recovering from HCT at a greatly increased risk of acquiring pathogens in their gut microbiome.

Results

Sample characteristics and patient geography

We collected weekly stool samples (see methods) from adult patients undergoing hematopoietic cell transplantation (HCT) at Stanford University Medical Center from 2015-2019. At the time of the study, our biobank contained over 2000 stool samples from over 900 patients. Samples from October 2015 to November 2018 were considered for this study. Relevant patient health, medication, demographic, hospital admission and room occupancy data were extracted from electronic health records (Table 1, Table S1). All patients stayed in a single ward of the hospital during treatment, which contained 14 single-occupancy and four double-occupancy rooms, the latter of which included shared bathrooms (Figure S1a). Patients spent a median of 18 days on the ward and were frequently moved between rooms: 42% of patients spent at least one day in three or more rooms during the course of treatment (Table 2, Figure S1c). 73% of patients shared a room with a roommate for ≥ 24 hours. Over the course of their hospital stays, many patients had several roommates, though never more than one at a time (Figure S1d).

To understand how geographic overlap may influence transmission of gut microbes, we created a network from patient-roommate interactions (Figure S1b). 535 patients (77% of patients with at least one roommate, 56% of all patients) fell into the largest connected component of the network. Although the largest component was not densely connected (mean degree 2.2 ± 1.6 standard deviation (SD)), it links together patients over three years and may represent a risk for infection transmission. We used the network to select samples for further analysis with metagenomic sequencing, as described in the methods.

Metagenomic sequencing, assembly and binning

For an overview of the steps used in the generation and processing of sequence data, see Figure 1a. 328 stool samples from 94 HCT patients were subject to short-read metagenomic sequencing as part of previous projects (for references and SRA IDs of these samples, see Table S2). 96 additional samples

from 62 patients were selected for linked-read sequencing to span periods of roommate overlap between patients. Samples were subjected to bead beating-based DNA extraction and bead-based DNA size selection for fragments ≥ 2 kb (see methods). We prepared linked-read sequencing libraries with the 10X Genomics Chromium platform from 89 samples with sufficient DNA concentration. Samples were sequenced to a median of 116 million (M) (± 37 M SD) read pairs on an Illumina HiSeq4000. In total, 401 stool samples from 149 patients were sequenced (Table 3), with a median of 2 and maximum of 13 samples per patient (Figure 1b).

We processed all existing short-read data and newly generated linked-read data by first trimming and then removing low quality reads, PCR duplicates (short-read data only) and reads that aligned against the human genome (see methods). After quality control, newly sequenced linked-read samples had a median 104 M (± 40 M SD) read pairs, while short-read data had a median 7.6 M (± 4.4 M SD) read pairs. Metagenomic assembly was conducted using metaSPAdes³⁰ for short-read data, and MEGAHIT³¹ followed by Athena²⁶ for linked-read data. Short-read assemblies had a median N50 of 17.2 kb \pm 24.8 kb, while linked-read assemblies had a median N50 of 147.6 \pm 165.8 kb. We binned metagenome-assembled genomes (MAGs) using Metabat2³², Maxbin³³ and CONCOCT³⁴ and aggregated across results from each tool using DASTool³⁵. MAG completeness and contamination was evaluated using CheckM³⁶ and MAG quality was determined by previously established standards³⁷. The vast majority of short-read and linked-read MAGs were at least medium quality, and 27% of linked-read MAGs contained the 5S, 16S and 23S rRNA genes and at least 18 tRNAs to be considered high-quality (Figure 1c, Table S3). Linked-read MAGs had higher quality than the 4,644 species-level genomes in the Unified Human Gastrointestinal Genome collection³⁸, where 573 genomes (12.3%) are high-quality, and only 38 (6.6%) of those came from metagenomes rather than isolates. Sequencing dataset type (short-read vs linked-read) did not have a linear relationship with MAG length (linear regression, $p > 0.9$); the increase in quality was mainly due to the inclusion of ribosomal and transfer RNA genes in the linked-read MAGs, which often do not assemble well with short-read sequencing data alone.

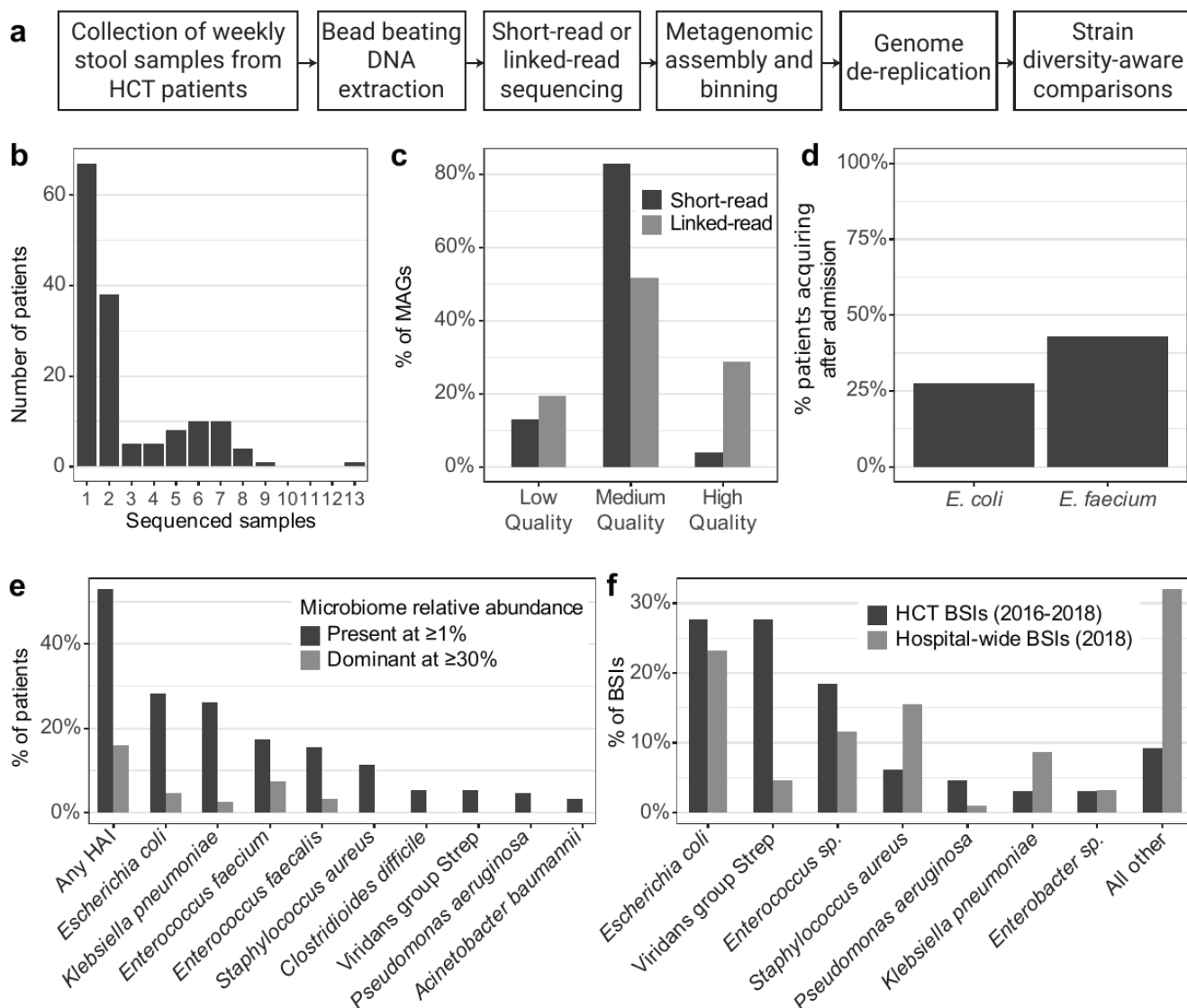


Figure 1: Overview of the methods, data generated, and clinical features of this sample set.

a) Overview of the experimental and computational workflow used to generate sequencing datasets, bin MAGs and compare strains between patients.

b) Number of stool samples sequenced per patient.

c) Percentage of MAGs meeting each quality level³⁷, stratified by sequencing method.

d) Of patients who have the given organism present ($\geq 1\%$ relative abundance) in a time course sample, percentage of patients who likely acquired the organism after admission to the hospital ($<0.1\%$ relative abundance in the first sample). *E. coli*, $n = 8/29$ patients; *E. faecium*, $n = 9/21$ patients.

e) Percentage of patients with at least one sample positive with ($\geq 1\%$ relative abundance) or dominated by ($\geq 30\%$ relative abundance) hospital acquired infection (HAI) organisms, as identified by Kraken2- and Bracken-based classification.

f) Percentage of bloodstream infections (BSIs) identified with each organism or group in HCT patients and hospital-wide.

Classification of Healthcare-associated Infection organisms

We performed taxonomic classification of sequencing reads with Kraken2³⁹ and abundance estimation with Bracken⁴⁰ using a custom database of bacterial, fungal, archaeal and viral genomes in NCBI Genbank (see methods) (Table S4, S5). A median of 33% \pm 15% SD reads were classified to the species level with Kraken2 (72% \pm 15% SD at the genus level), which was improved to 96% \pm 7% SD using Bracken (97% \pm 8% SD at the genus level). Organisms that cause healthcare-associated Infections (HAI) were identified from the CDC list of pathogens⁴¹. Determining true presence or absence of an organism in a metagenomic sequencing sample is difficult and is confounded by sequencing depth, misclassification errors and other biases. We used a relative abundance threshold of 1% of sequencing reads classified to the species level by Bracken to establish presence as this represents a coverage regime where we can reliably assemble high-quality genomes with linked-read sequencing.

Many HAI organisms were prevalent in the microbiomes of the studied HCT patients. 152 samples (38%) from 79 patients (53%) had at least one HAI organism identified at 1% relative abundance or above (Figure 1e). *Escherichia coli* was the most common HAI organism (present at \geq 1% in 42/149 patients, 28.2%; 0.1%=80/149, 53.7%), followed by *Klebsiella pneumoniae* (39/149 patients, 26.2%; 0.1%=70/149, 47%) and *Enterococcus faecium* (26/149 patients, 17.4%; 0.1%=73/149, 49%). Rates of colonization with HAI organisms were much higher than in stool samples from healthy individuals in the Human Microbiome Project⁴² where *E. coli* reaches 1% relative abundance in 2.1% of samples, and *K. pneumoniae* and *E. faecium* are never found at greater than 1% (present at 0.1% in 18.4%, 1.4% and 0.7% of samples, respectively). HCT patient microbiomes can become dominated by HAI organisms, often as a result of antibiotic usage. 24 patients (16%) have at least one sample with a dominant HAI organism (\geq 30% relative abundance), which may place them at increased risk for bloodstream infections (BSI)⁶. BSI in this cohort of HCT patients is most frequently caused by *E. coli*, viridans group Streptococci and *E. faecium*; these organisms less frequently cause BSI among the entire inpatient population at our hospital (Figure 1f). We focused further analysis on *E. coli* and *E. faecium*, as these species are both frequently detected in stool and frequently cause BSIs. While viridans group

Streptococci frequently cause BSIs in HCT patients, these species are typically much more prevalent in the oral cavity^{2,43} compared to the gut microbiome (individual species in the group only reach 1% relative abundance in 8/149 patients, 5%).

HAI organisms can be acquired during the hospital stay

We investigated patients with time course samples (82/149 patients, 55%) to determine if HAI organisms were acquired during the observed hospital stay. *E. coli* was present ($\geq 1\%$ relative abundance) in the microbiome of 29 patients with at least two sequenced samples. In 8/29 (28%) patients, *E. coli* was undetected (relative abundance $< 0.1\%$) in the first sample from the patient (Figure 1d). *E. faecium* was present in the microbiome of 21 patients with at least one sample, including one patient with 0.4% relative abundance but a high-quality MAG, which was therefore included. In 9/21 (43%) patients, *E. faecium* was undetected (relative abundance $< 0.1\%$) in the first sample from the patient. Although 11 patients with time course samples had both *E. coli* and *E. faecium* present in at least one sample at $\geq 1\%$, none of these patients appear to have acquired both organisms during their hospital stay. Our findings indicate that a fraction of patients may acquire either *E. coli* or *E. faecium* in the microbiome during the hospital stay. The difference in the fraction of patients acquiring each organism was not statistically significant ($p=0.27$, likelihood ratio test).

HAI organisms that colonize HCT patient microbiomes are part of known, antibiotic resistant and globally disseminated clades

E. coli and *E. faecium* are common commensal colonizers of human microbiomes^{44–46}. These species can also be pathogenic and contribute to inflammation, dysbiosis and infection in the host⁴⁷. The specific strain of these species is key in determining the balance between a healthy and diseased state in the microbiome. To understand the diversity of strains present in the microbiomes of our patients, we clustered all medium- and high-quality MAGs at 95% and 99% identity thresholds (roughly “species” and “strain” level, see methods) using dRep⁴⁸, yielding 1615 unique genomes representative of the microbial diversity in this sample set. We then included several *E. coli* and *E. faecium* strains reference genomes

(Table S6) in the comparison to identify the closest strains or sequence types compared to the patient-derived MAGs.

Escherichia coli

The 95% identity, or species-level, cluster of *E. coli* MAGs contained 47 genomes from 26 patients (Figure 2). Within this alignment average nucleotide identity (ANI) based tree, we observed two clades of genomes where MAGs from multiple patients had >99.9% ANI. These clades were investigated further as they may represent common sequence types. The first clade contained 15 MAGs from 7 patients; these MAGs had >99.9% ANI to pathogenic *E. coli* sequence type (ST) 131 clade C2 genomes, including EC958⁴⁹ and JJ1886⁵⁰. ST131 is an extraintestinal, pathogenic, multidrug resistant *E. coli* strain which frequently causes urinary tract infections⁵¹. *E. coli* ST131 often carries extended-spectrum β -lactamase (ESBL) genes which convey a wide range of antibiotic resistance. This sequence type is believed to colonize the intestinal tract even in healthy individuals without antibiotic exposure⁵², and there are reports of this pathogen causing urinary tract infections in multiple individuals within a household⁵³.

The second clade contained 12 MAGs from 5 patients with >99.8% ANI to the pathogenic ST648 representative IMT16316⁵⁴. ST648 is also an ESBL-producing *E. coli* strain, but it is not as widespread as ST131. Both STs have been isolated from wastewater⁵⁵ and ST648 has been isolated from the gut of humans⁵⁶ and other mammals⁵⁷. Our finding that *E. coli* ST648 is also prevalent in HCT patient microbiomes suggests that it may become a pathogen of interest in this patient population in the future.

To understand the antibiotic resistance capabilities of the *E. coli* strains colonizing these HCT patients, we searched for β -lactamase genes in the *E. coli* MAGs (see methods). The most commonly detected genes were *ampH* and *ampC*, which are part of the core *E. coli* genome and likely do not contribute to antibiotic resistance⁵⁸ (Figure S2A). CMY-132 was detected exclusively in MAGs in the ST131 clade, and mutations conveying resistance in *gyrA* were detected in MAGs in multiple clades. CTX-M-type β -lactamases were detected in several samples, but often within the metagenome rather than within the *E. coli* MAG, indicating they may be on plasmids or mobile genetic elements that did not bin with the rest of the *E. coli* genomes.

Escherichia coli



Figure 2: Alignment average nucleotide identity (ANI) tree of *Escherichia coli* MAGs. MAGs identified as *E. coli*, medium quality or above and at least 75% the mean length of the reference genomes are included. Several reference genomes are included and labeled with an asterisk. Clusters at the 99% ANI level corresponding to ST131 (purple) and ST648 (orange) are highlighted. Alignment values used to construct this tree can be found in Table S7.

Enterococcus faecium

The species-level cluster of *E. faecium* MAGs contained 30 genomes from 20 patients (Figure 3a). All MAGs were $\geq 99\%$ identical, suggesting a single ST is present in most patients⁴⁵. These genomes matched closest to *E. faecium* ST117, a well-described vancomycin-resistant strain that frequently causes bloodstream infections⁵⁹. Notably, five other MAGs had $\sim 94\%$ ANI (below the 95% clustering threshold, and therefore not shown in Figure 3a) to the ST117 clade and $>99\%$ ANI to commensal *E. faecium* strains, including strains Com15 and Com12⁴⁵. To understand the vancomycin resistance capabilities of these strains, we searched for the seven genes in the *vanA* operon⁶⁰. Only 2/30 linked-read samples had the full operon present within the *E. faecium* MAG (Figure S2b). However, when we looked in the entire metagenome, 22/30 samples had the full operon present, and the *vanA* genes were usually detected on a contig that was not assigned to any MAG. *Van* genes are often carried on mobile genetic elements or plasmids in *E. faecium*. These elements do not assemble well due to their repetitive nature, and are often challenging to assign to MAGs.

Interestingly, no *van* genes are present in sample 11342_02, but the full operon is present in 11342_03, collected 14 days later from the same patient. The *van* genes are also absent in a sample from another patient (11349_01) with a nearly identical *E. faecium* strain that was found after the patients shared a room for 11 days. In sample 11342_03, the *vanA* operon appears on a contig 8.7 kb in length and is contained in the *E. faecium* MAG. However, coverage of *vanA* operon was approximately 1% of the coverage in the rest of the *E. faecium* MAG. Mapping reads against this contig revealed scattered coverage in 11342_02, leading us to believe the operon is present, but not at high enough coverage to be assembled in the earlier sample. A translated basic local alignment search tool (BLAST)⁶¹ search revealed that the final 1.2 kb, of this contig, directly after the *vanA* operon, is identical to an insertion sequence (IS) 256 family transposase. IS256 is a family of mobile genetic elements found in virulent *Enterococcus* and *Staphylococcus*^{62–64} which can mediate the transfer of resistance genes. Given the relatively low coverage of the *vanA* operon, and the fact that *Staphylococcus aureus* is present at 2.4%, 0.7% in samples 11342_02 and 11342_03 respectively, we believe that the *vanA* operon may be carried

in an organism such as *Staphylococcus aureus* in this sample, as opposed to *E. faecium*. Investigation with other methods, such as isolation culture, are necessary to determine which organism carries the *vanA* operon, as well as its impact on vancomycin resistance in this particular strain.

Nearly identical strains indicative of putative patient-patient *Enterococcus faecium*, but not *Escherichia coli* transmission

Although alignment-based MAG comparison is useful to understand genome structure and compare MAGs with reference strains, the method does have several drawbacks. MAGs are often incomplete, contain assembly and binning errors (particularly in low coverage or repetitive regions) and do not represent the high level of strain diversity present in microbiome communities⁶⁵. MAGs often fail to include plasmids, which play important roles in bacterial virulence and antibiotic resistance. To conduct a more sensitive analysis, we used the strain diversity-aware, SNP-based method inStrain⁶⁶. InStrain compares alignments of short reads from multiple samples to the same reference genome and reports two metrics: Consensus ANI (conANI) and Population ANI (popANI). ConANI counts a SNP when two samples differ in the consensus allele at a position in the reference genome, similar to many conventional SNP calling methods. PopANI counts a SNP only if both samples share no alleles. For example, if A/T alleles were found at frequencies of 90/10% and 10/90% in two samples, a consensus SNP would be called because the consensus base is different. A population SNP would not be called because both samples share an A and T allele. To determine a threshold for putative transmission between patients, we examined comparisons in several “positive control” datasets where we expect to find identical strains, either as the result of persistence or transmission: time course samples from the same HCT patient, stool samples from mother-infant pairs¹⁸ and samples from fecal microbiota transplantation donors and recipients⁶⁷. We often observed 100% popANI in these “positive control” comparisons, indicating that there were no SNPs that could differentiate the strain populations in the two samples (Figure S3, S4). Due to expected noise and errors in sequencing data, we set the lower bound for transmission in our HCT cohort at 99.999% popANI, equivalent to 30 population SNPs in a 3 megabase (Mb) genome. The same threshold was used to classify two strains as the same by the authors of inStrain⁶⁶.

Escherichia coli

We compared all samples where *E. coli* was covered $\geq 5x$ for $\geq 50\%$ of the genome in both samples, including samples where we did not assemble an *E. coli* MAG. While *E. coli* genomes in

samples collected from the same patient over time were always more similar than the putative transmission threshold, in no case did we observe a pair of samples from different patients with $\geq 99.999\%$ popANI (Table S8). This result suggests that all *E. coli* strains observed are patient-specific, and argues that there are no common strains that are circulating in the hospital environment or passing between patients. Alternatively, patient-patient transmission or acquisition of common environmental strains is either notably rare or rapid genetic drift after a patient acquires a new strain is reducing popANI levels below the threshold. Deeper metagenomic sequencing or isolation and sequencing of *E. coli* strains may allow us to detect transmission in previously missed cases.

Enterococcus faecium

We performed the same analysis in *E. faecium* and observed four examples where two patients shared a strain with $\geq 99.999\%$ popANI (Figure 3b,c). In one case, the two patients were roommates and direct transmission appears to be the most likely route. In the other three cases, epidemiological links were less clear, suggesting the patients may have acquired a similar strain from the hospital environment or through unsampled intermediates. In the following descriptions, samples are referred to by the day of collection, relative to the first sample from patients in the comparison.

Case 1: Patients 11342 and 11349 overlapped in the ward for 21 days and were roommates for 11 days (Figure 4a). Patient 11342 had a gut microbiome that was dominated by *E. faecium*; the two samples from this patient have 60% and 87% *E. faecium* relative abundance. A single sample from patient 11349 was obtained 14 days after starting to share a room with patient 11342. This sample is dominated by *Klebsiella pneumoniae*, and *E. faecium* is at 0.4% relative abundance. InStrain comparisons between the *E. faecium* strains in 11342 (the presumed “donor”) and 11349 (the presumed “recipient”) of the strain revealed 0-2 population SNPs (popANI 100% - 99.9999%) with 87% of the reference MAG (2.24 Mb) covered $\geq 5x$ in both samples. MAGs from each patient were also structurally concordant (representative dotplots in Figure S6a). These genomes were the most similar out of all *E. faecium* genomes compared from different patients. Samples from these patients were extracted in different batches and sequenced on different lanes, minimizing the chance sample contamination or

“barcode swapping”⁶⁸ (see Supplemental Note) could be responsible for this result. No other strains were shared between these two patients.

Case 2: Patients 11575 and 11568 overlapped on the ward for 36 days but were never roommates (Figure 4b). Samples from patient 11575 span 97 days, during which this patient experienced a BSI with *Klebsiella pneumoniae*, a concomitant reduction in microbiome diversity and microbiome domination by *E. faecium* in samples collected on days 16 and 28. Two samples were collected from patient 11568 on days 28 and 119. The first sample from 11568 was also dominated by *E. faecium*, but strains from the two patients were distinct (99.95% popANI). 91 days later, the second sample from 11568 has a lower relative abundance of *E. faecium* but a nearly identical strain to patient 11575. Five population SNPs (99.9997% popANI) were detected with 88% of the reference MAG covered $\geq 5x$ in both samples (representative dotplot Figure S6b). This suggests that the *E. faecium* strain in 11568 was replaced by a different strain with high identity to the strain in 11575. Patient 11568 was discharged from the HCT ward during the period between the two samples. The shared strain may represent an acquisition from a common environmental source or transmission from unobserved patients, rather than a direct transmission event between these two patients. While the *E. faecium* strain was different at the two time points from patient 11568, an *E. faecalis* strain remained identical.

Case 3: Patients 11605 and 11673 did not overlap in the ward (Figure 4c). Two samples were collected from 11605 on days 0 and 14. This patient experienced a BSI with *E. faecium* prior to a sample dominated by the same species on day 14. Patient 11673 experienced a BSI with *E. coli* prior to the single sample we collected from this patient. Comparing *E. faecium* strains between the two patients revealed 2 population SNPs (99.9998% popANI) with 48% of the reference MAG covered $\geq 5x$ in both samples (representative dotplot Figure S6c). Although slightly below the 50% coverage threshold, the high degree of similarity caused us to consider this result. While *E. faecium* strains in the two patients were nearly identical, the samples were collected 161 days apart and the patients had no overlap in the ward. This suggests both patients may have acquired the strain from the hospital environment, through transmission from unsampled patients, or another source such as healthcare workers.

Case 4: Patients 11360 and 11789 did not overlap in the ward. *E. faecium* remained at relatively low abundance in all samples. Comparing *E. faecium* strains between patients revealed 5-10 population SNPs (99.9993% - 99.9996% popANI) with 50%-57% genome coverage. Neither patient had a BSI during the sampling period. As these samples were collected at least 428 days apart, a shared source again may be the most likely explanation.

Comparisons with *E. faecium* and *E. coli* in published data

The *E. faecium* and *E. coli* strains we observe in our patients may be unique to this patient population and hospital environment. Alternatively, they may be hospital acquired strains that are present in other settings around the globe. We searched through several published datasets to differentiate between these possibilities. Our comparison dataset included metagenomic shotgun sequence data from 189 stool samples from adult HCT patients⁶⁹, 113 stool samples from pediatric HCT patients^{3,70,71}, 732 stool samples from hospitalized infants⁷² and 58 vancomycin-resistant *E. faecium* isolates⁷³. Sequence data were downloaded from SRA and processed in the same manner as other short-read data. Each sample was aligned against the *E. faecium* and *E. coli* MAGs used in the inStrain analysis above, profiled for SNPs, and compared against samples collected from our HCT patients. Comparisons within our data and comparisons within individual external datasets frequently achieved popANI values of $\geq 99.999\%$, typically from comparisons of samples from the same patient over time. Meanwhile, comparisons between our samples and external samples had lower popANI values (Figure S5).

Comparisons of *E. faecium* strains in samples from patient 11346 in our dataset and patient 688 in the HCT microbiome dataset collected at Memorial Sloan Kettering Cancer Center⁶⁹ demonstrated a maximum of 99.9993% popANI (16 population SNPs detected in 2.3 Mb compared). While direct transmission is likely not involved here, this observation does align with the nearly identical *E. faecium* strains we observed in patients with no geographic or temporal overlap (case 3 and 4) and speaks to the global dissemination of vancomycin-resistant *E. faecium* ST 117. Comparing *E. coli* to external datasets revealed a maximum of 99.996% popANI (200 population SNPs detected in 5.0 Mb compared).

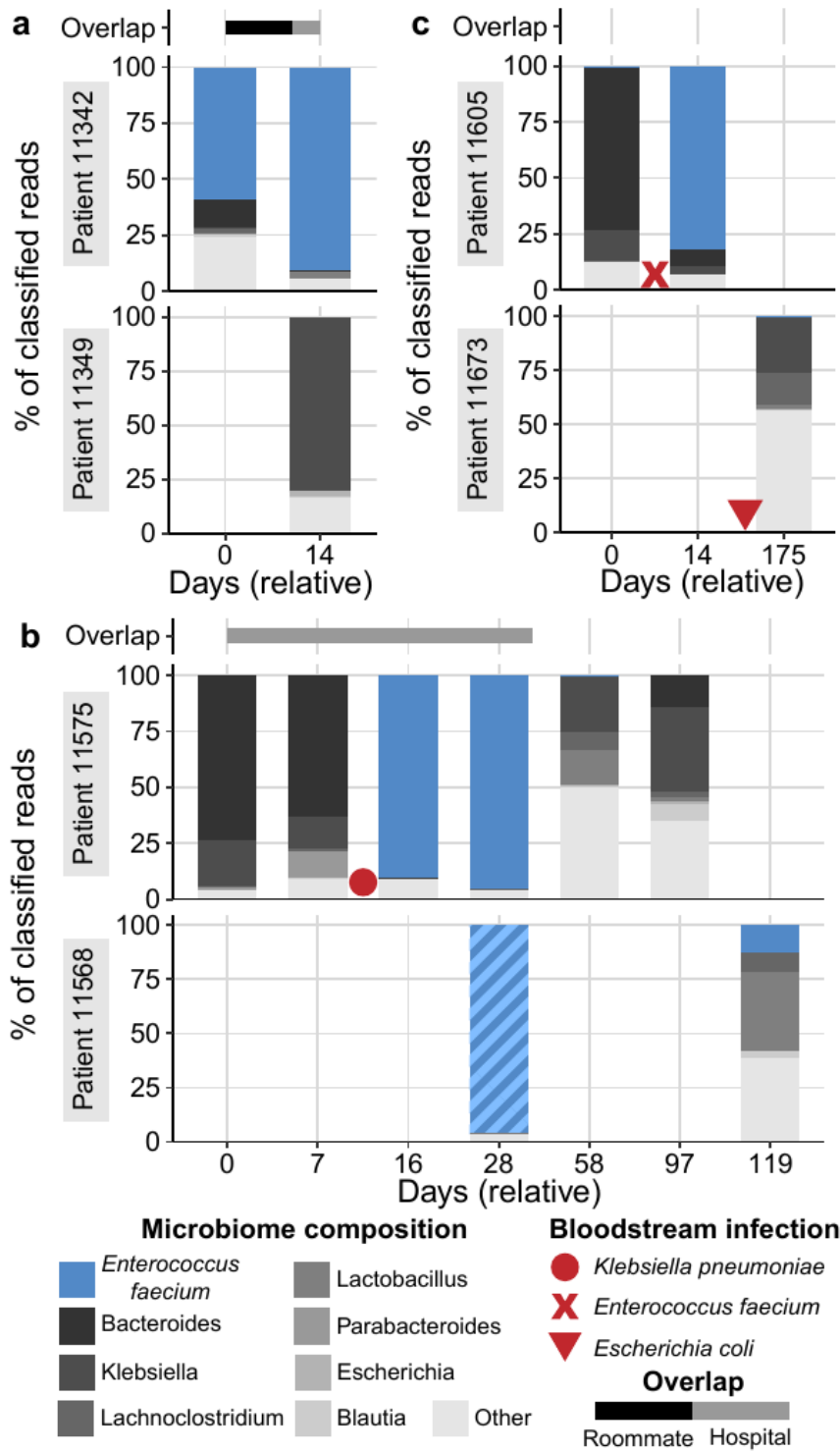


Figure 4: Microbiome composition of patients with putative *Enterococcus faecium* transmission events. Each panel shows the composition of two patients over time. The height of each bar represents the proportion of classified sequence data assigned to each taxon. Samples are labeled relative to the date of the first sample in each set. Bars above each plot represent the approximate time patients spent in the

same room (black bars) or in the hospital (grey bars). Red symbols indicate approximate dates of bloodstream infection with the specified organism. Hypothesized direction of transmission progresses from the top to the bottom patient. Fractions of the bar with >99.999% popANI strains in each panel are indicated with solid colors, and different strains are indicated with hashed colors. All taxa except *E. faecium* are shown at the genus level for clarity.

- a) Case 1: Putative transmission from patient 11342 to 11349.
- b) Case 2: Putative transmission from patient 11575 to 11568.
- c) Case 3: Putative transmission from patient 11605 to 11673.

Putative transmission of commensal bacteria

Next, we extended the inStrain analysis to compare all species that were present in multiple patients. We found nearly identical genomes of commensal organisms that may be the result of transmission between patients, as well as several species shared between patients without clear explanations.

Hungatella hathewayi

Patients 11639 and 11662 overlapped in the ward for 34 days and were roommates for a single day, after which 11639 was discharged (Figure 5a). *Hungatella hathewayi* was at 5-10% relative abundance in the two samples from 11639. Patient 11662 developed *Streptococcus mitis* BSI on day 24. The microbiome of this patient recovered with markedly different composition, including an abundant *H. hathewayi* strain reaching 54% and 17% relative abundance on days 58 and 100, respectively. Comparing *H. hathewayi* genomes between these two patients revealed 0-1 population SNPs (100% - 99.99998% popANI) with 94%-98% coverage $\geq 5x$ (6.9 - 7.1 Mb sequence covered in both samples). This was the single highest ANI comparison among all strains shared between patients. *H. hathewayi* MAGs from these patients were also structurally concordant and had few structural variations (Figure S6d). No other strains were shared between these patients.

Patient 11662 had *H. hathewayi* in the first two samples at 1.2% and 0.3% relative abundance, respectively. Although we were limited by coverage, comparing early to late samples with inStrain revealed 472 population SNPs in 3% of the genome that was covered at least 5X, implying 11662 was initially colonized by a different *H. hathewayi* strain, which was eliminated and subsequently replaced by the strain present in 11639. Given that samples were collected weekly, determining the direction of transmission is challenging. However, 11639 to 11662 appears to be the most likely direction, given the sampling times and perturbation 11662 experienced. However, it is possible that transmission occurred in the opposite direction or from a common source. Interestingly, 11662 was also re-colonized with *Flavonifractor plautii* in later samples. This strain was different from the strain in earlier samples from this patient, as well as all other *Flavonifractor* strains in our sample collection.

H. hathewayi is known to form spores and is able to persist outside a host for days⁷⁴. Although these patients were only roommates for a single day, 11662 remained in the same room for 4 days after 11639 was discharged, increasing the chance that a *H. hathewayi* spore could be transmitted from a surface in the shared room or bathroom. The question remains as to why transmission of *H. hathewayi* is not more common, given it is found at $\geq 1\%$ relative abundance in 31 patients. Perhaps the earlier colonization of the microbiome of 11662 with a different *H. hathewayi* strain was key - the microbiome in this patient was “primed” to receive a new strain of the same species, despite the significant perturbation this patient experienced.

Notably, *H. hathewayi* was recently reclassified from *Clostridium hathewayi*⁷⁵, and was previously shown to induce regulatory T-cells and suppress inflammation⁷⁶. Although the interaction of this microbe in HCT is not known, it may be interesting to investigate further given that the microbe may be transmitted between individuals and may contribute to inflammation suppression that may be relevant in diseases such as graft-vs-host disease. However, *H. hathewayi* may not be entirely beneficial or harmless and has been reported to cause BSI and sepsis in rare cases^{77,78}.

Akkermansia muciniphila

Patients 11742 and 11647 overlapped in the ward for 11 days and were roommates for nine days (Figure 5b). Patient 11647 experienced a BSI with *Klebsiella pneumoniae* (perhaps related to previous *K. pneumoniae* domination of the microbiome). The final sample from 11647 has *Akkermansia muciniphila* at 9.4% relative abundance, while the single sample from 11742 was dominated by *A. muciniphila* (85% relative abundance). Comparing these genomes revealed 0 population SNPs and 7 consensus SNPs with 90% coverage, as well as concordant MAGs from each sample (Figure S6e). No other strains were shared between these two patients.

In contrast to *H. hathewayi*, *A. muciniphila* is not known to form spores, which may reduce the chance of this microbe being transmitted. However, it is an aerotolerant anaerobe that may survive in oxygen for short periods of time⁷⁹. The microbiome domination of 11742 with *A. muciniphila* and the

relatively long overlap period of nine days in the same room may provide a greater “infectious dose” (abundance * exposure time) to the recipient patient.

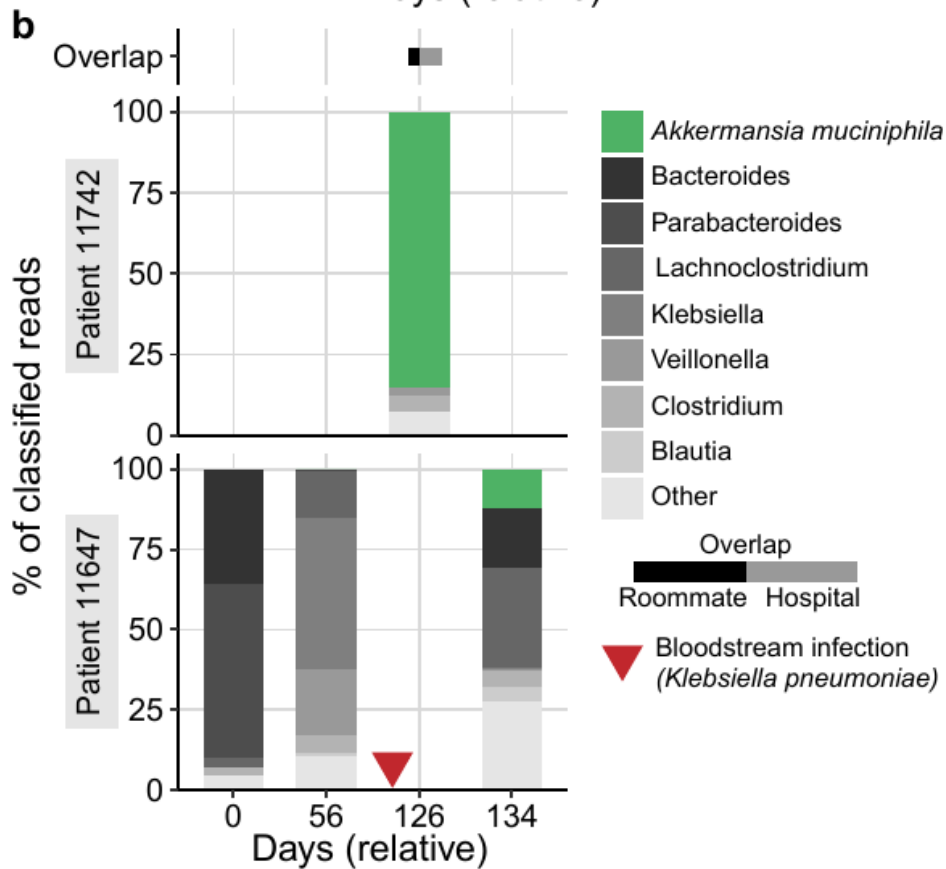
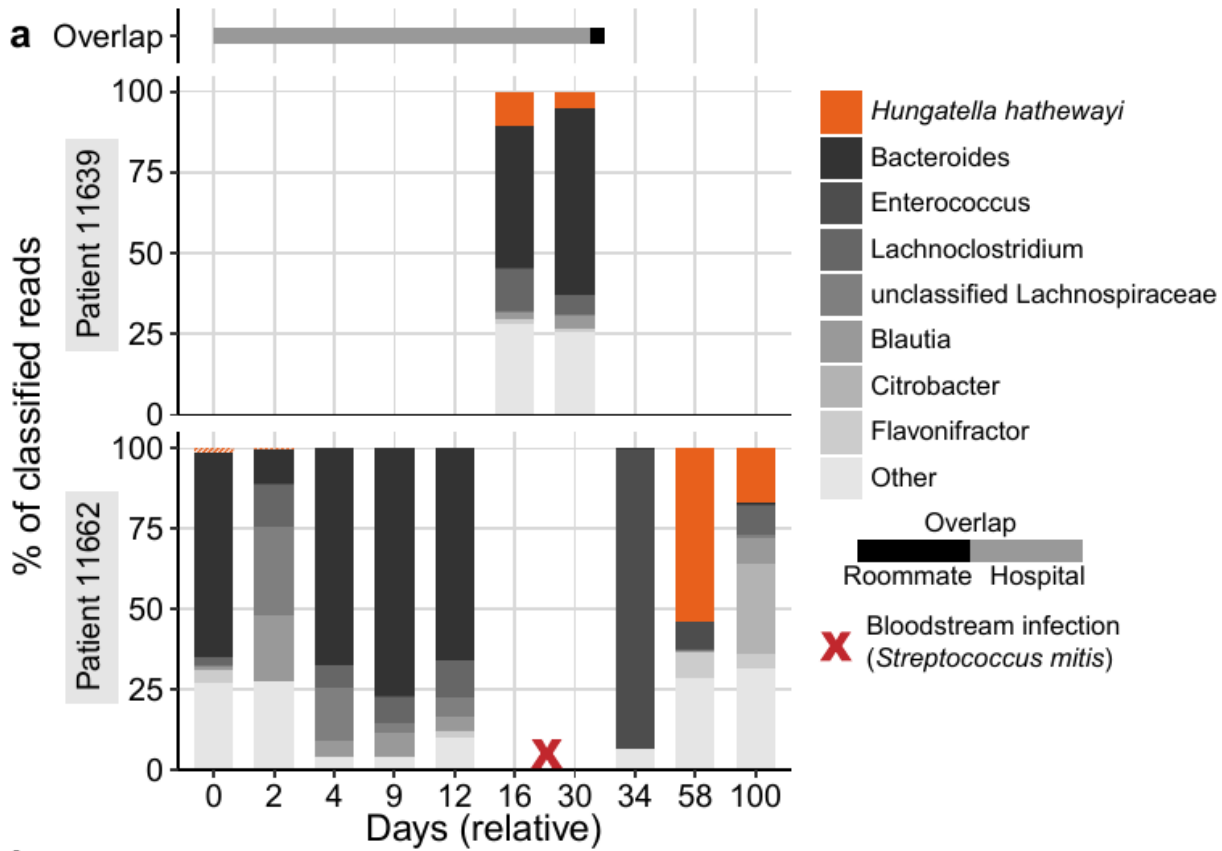


Figure 5: Microbiome composition of patients with putative *Hungatella hathewayi* or *Akkermansia muciniphila* transmission events. Each panel shows the composition of two patients over time. The height of each bar represents the proportion of classified sequence data assigned to each taxon. Samples are labeled relative to the date of the first sample in each set. Bars above each plot represent the approximate time patients spent in the same room (black bars) or in the hospital (grey bars). Red symbols indicate approximate dates of bloodstream infection with the specified organism. Hypothesized direction of transmission progresses from the top to the bottom patient. Fractions of the bar with >99.999% popANI strains in each panel are indicated with solid colors, and different strains are indicated with hashed colors. All taxa except *H. hathewayi* or *A. muciniphila* are shown at the genus level for clarity.

- a) Putative case of *H. hathewayi* transmission from 11639 to 11662.
- b) Putative case of *A. muciniphila* transmission from 11742 and 11647.

Widespread strain sharing of commercially available probiotic organisms

Several organisms were found with identical or nearly identical genomes across multiple patient microbiomes without clear epidemiological links. The largest clade was found for *Lactobacillus rhamnosus*, which included 11 samples collected from eight patients over a span of 2.5 years (Figure 6A,6D). All 11 samples in this clade had pairwise popANI of $\geq 99.999\%$, and in a subset of eight samples from seven patients, all pairs were identical from a popANI perspective (100%). Of the eight patients in this clade, only two pairs were roommates or overlapped in the hospital (patients 11537/11547 and 11647/11662, roommates for three days and one day, hospital overlap for 20 and 44 days, respectively). All 11 samples in this clade were collected after HCT (median time from HCT to first sample 43 days, range 12-93 days), and *L. rhamnosus* always had $<0.1\%$ relative abundance in pre-HCT samples, when present. Five of eight patients were discharged from the hospital after HCT and prior to acquiring *L. rhamnosus*, which we observed in a sample collected during a subsequent admission. We also observe *L. rhamnosus* falling below 0.1% relative abundance in a subsequent sample in five patients, suggesting that this strain may be a transient colonizer of the microbiome (example in Figure 6E). Similar clades of high-identity genomes from different patients were found for *Lactobacillus gasseri* (Figure 6B) and *Streptococcus thermophilus* (Figure 6C).

Given that we did not observe hospital or roommate overlap between most patients in the *L. rhamnosus* cluster, the most likely explanation is that patients acquired this strain from a common source. *L. rhamnosus* is a component of several commercially available probiotic supplements, is present in certain live active-culture foods such as yogurt, and is among the most commonly prescribed probiotic species in US hospitals⁸⁰. However, HCT recipients were not allowed to take probiotics or consume high-bacteria dairy products, such as probiotic yogurt or soft cheese, while inpatients on the HCT ward. We also verified that no prescriptions were written for probiotics by examining electronic health records. A majority of patients were discharged from the hospital between HCT and acquiring the *L. rhamnosus* strain, which may have provided them with the opportunity to consume a probiotic

supplement or dairy product. Contact with a family member or other individual who had the strain in their microbiome could also be responsible for colonization of the HCT patient.

If this *L. rhamnosus* strain is a commonly used probiotic supplement or is found in commonly consumed dairy products, it may be found in other gut microbiome sequencing datasets. Comparing MAGs from this cluster against all Genbank genomes revealed a maximum alignment-based ANI of 99.95% to *L. rhamnosus* ATCC 8530⁸¹. Instrain-based comparisons against this reference had a maximum popANI of 99.98%, below the putative transmission threshold. We then searched against all genomes in the Unified Human Gastrointestinal Genome collection³⁸ and identified two genomes that were nearly identical to the strain found in HCT patients. These genomes were originally from the Human Gastrointestinal Bacteria Culture Collection⁸² (accessions ERR2221226 and ERR1203919, belonging to the same isolate per a personal communication with the authors). Assembled isolate and patient-derived genomes had $\geq 99.99\%$ ANI; inStrain-based SNP comparisons had $\geq 99.999\%$ popANI. This suggests that a *L. rhamnosus* strain that is nearly identical to the genomes in our HCT patients has been isolated from human stool in the past.

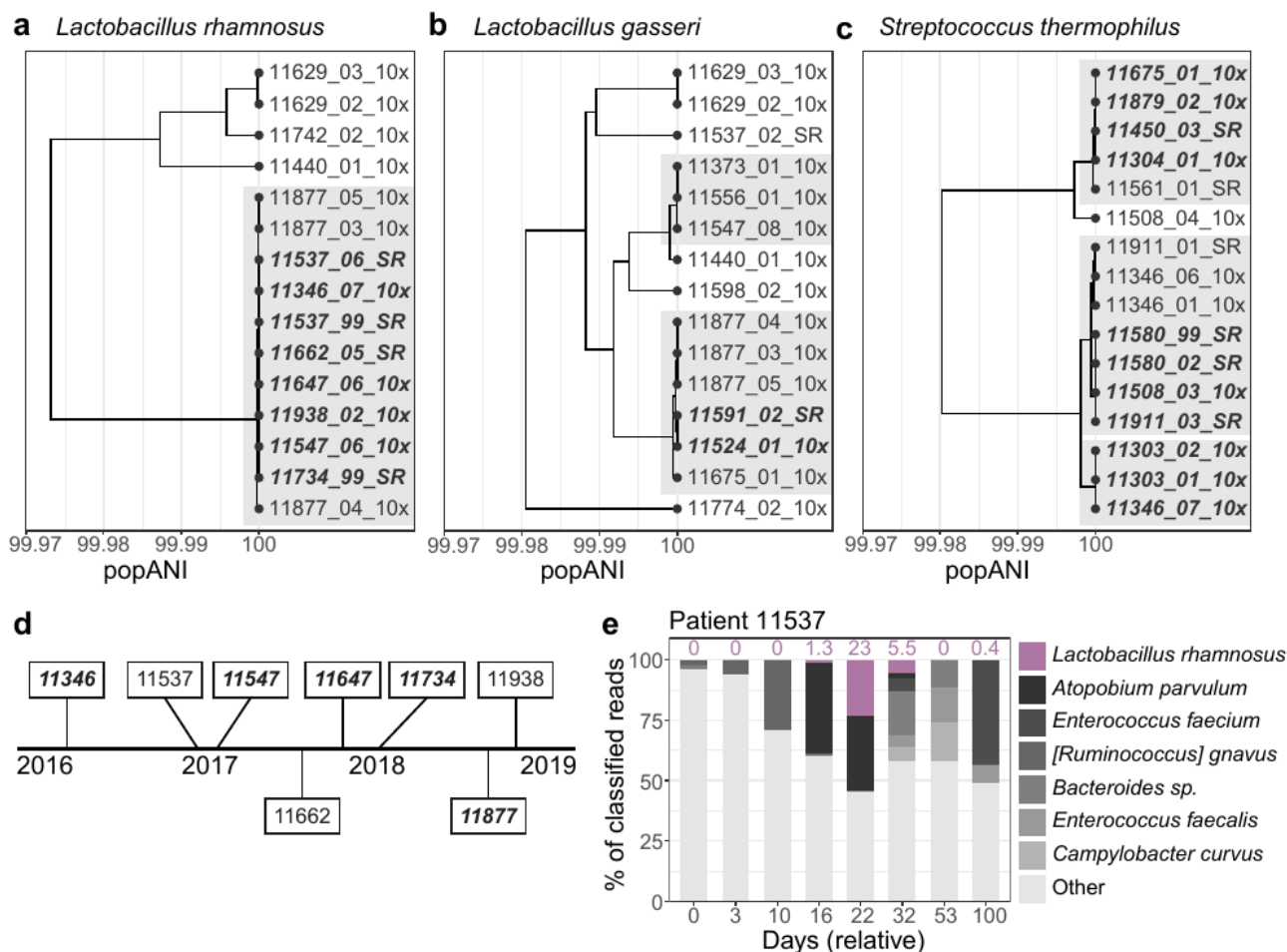


Figure 6: *Lactobacillus* and *Streptococcus* strains are acquired after HCT and identical between many patients.

Population ANI based tree of (a) *Lactobacillus rhamnosus*, (b) *Lactobacillus gasseri*, (c) *Streptococcus thermophilus* strains present in patient samples. Clades containing samples from different patients with $\geq 99.999\%$ popANI are highlighted with a grey background. Clades with 100% popANI between all pairs are additionally bolded and italicized.

d) Timeline of approximate date of samples containing a *L. rhamnosus* strain in the transmission cluster in (a). Patients who were discharged from the hospital after HCT and prior to acquiring *L. rhamnosus* are bolded and italicized.

e) Microbiome composition of patient 11537. *L. rhamnosus* abundance at each time point is indicated above the bar. This patient received HCT on relative day 3.

Discussion

Our investigation using high-resolution metagenomic sequencing attempts to quantify if and when patient-patient microbiome transmission is involved in the spread of pathogenic organisms. We first found that hospitalized HCT patients frequently harbor HAI organisms in their gut microbiome, validating previous studies which used culture-based approaches or 16S rRNA sequencing^{6,23,24}. MAGs created from patient samples had high identity to several globally disseminated and antibiotic resistant sequence types, including *Escherichia coli* ST131 and ST648. Interestingly, whereas ST131 is a well-recognized multi-drug resistant pathogen, ST648 is nearly as prevalent as ST131 in our sample collection, and may thus be an emerging pathogen in this patient population.

To measure putative transmission between human microbiomes with high levels of strain diversity²⁹ we used the program inStrain⁶⁶ and the strain diversity-aware metric population ANI (popANI). Although *E. coli* ST131 and ST648 were common colonizers of the microbiome of hospitalized HCT patients, we did not identify any pairs of patients harboring *E. coli* strains with popANI values above the 99.999% popANI transmission threshold. Taken together with the observation that *E. coli* is commonly present in the patient's microbiome upon admission, this finding argues that patients usually enter the hospital with an "individual-specific" *E. coli* strain and do not frequently transmit it to others. An exclusion principle may be at play, where an *E. coli* niche can only be filled by a single strain and new strains are unlikely to engraft when the niche is already occupied. In contrast to *E. coli*, we observed four pairs of patients with *E. faecium* strains that were more similar than 99.999% popANI. In one case, the two patients spent 11 days sharing a room and bathroom prior to observing the shared strain. Direct links between patients were less clear or non-existent in the other three cases, and transmission through unsampled intermediates or acquisition from an environmental source may have been responsible. We also found evidence for an *E. faecium* strain in a published dataset from HCT patient microbiomes⁶⁹ that had above 99.999% popANI to a strain in our sample collection. While this finding is likely not the result of patient-patient transmission, it does indicate that very similar strains may exist within patients in different geographic locations.

We then expanded the transmission analysis to examine all species that were present in the microbiome of multiple patients. Identical *Hungatella hathewayi* strains were found in two patients who were in the hospital together for 34 days and roommates for a single day. Earlier samples from patient 11662 had a significantly different *H. hathewayi* strain than the strain present in later samples. It is possible that the earlier colonization with the same species exhibited a priority effect⁸³ and primed this individual to be re-colonized. In another set of patients who overlapped in the hospital for 11 days and were roommates for nine days, we identified identical *Akkermansia muciniphila* strains. In both examples, the likely “recipient” patient experienced BSI prior to the putative transmission event. The subsequent antibiotic treatment initiated for the treatment of BSI resulted in vast microbiome modification and simplification, which may have opened a niche for the new organism to engraft into. Both *H. hathewayi* and *A. muciniphila* can survive outside the host for periods of time, but *H. hathewayi* can form spores that enable it to live in aerobic conditions for days⁷⁴. In the case of *H. hathewayi* transmission, patient 11662 remained in the same room with a shared bathroom after the single day of overlap with patient 11639. Spores surviving on surfaces may be responsible for transmission, given the relatively short period of overlap. In these cases, patient-patient transmission may help in the recovery of microbiome diversity following BSI and may play a role in ameliorating post-HCT inflammatory processes, such as acute graft-vs-host disease.

Finally, we observed identical probiotic species in multiple patients without clear geographic or temporal links, including *Lactobacillus rhamnosus*, *Lactobacillus gasseri*, and *Streptococcus thermophilus*. Acquisition from a commercially available probiotic or live-active culture food appears to be the most likely explanation. While patients hospitalized for HCT were not allowed to consume probiotics or high-bacterial dairy foods, a majority of patients were discharged after HCT and prior to a subsequent admission, upon which *L. rhamnosus* was detected. Many patients lost the strain in later samples, suggesting that *L. rhamnosus* was a transient colonizer. This matches the observation that abundance of probiotic species in the gut often declines after supplementation ends²⁰.

The healthy adult gut microbiome is relatively resistant to perturbation and colonization with new strains or species¹⁹. In contrast, mother-to-infant transmission of bacteria and phages is common and well-described^{16–18}. Patients in our study often shared spaces, were exposed to dramatic “niche clearing” therapies and were often immunosuppressed. We frequently observed patients acquiring new organisms into their gut microbiome during their hospital stay, especially following BSI. Still, we found that patient-patient transmission of gut microbes is relatively rare. This suggests that age, rather than perturbation or microbial exposure, may play the largest role in microbiome transmission. There are also several alternative explanations for the relative lack of transmission between patients. First, the adult gut microbiome may remain densely colonized even when dramatically perturbed by antibiotics and chemotherapy, and thus resistant to invasion with new strains. Strains we observed in later samples may have existed at low very levels in earlier samples from the individual, therefore evading detection. Second, it is possible that the microbiome of healthcare workers, hospital visitors, or other staff serve as the source of newly colonizing strains. Third, it is possible that the built environment, equipment used in the care of these individuals, and other environmental sources such as food and personal items harbored the microbes that were later transmitted. As we did not sample these other potential sources, it is difficult to know the extent to which they contributed to the collective reservoir of potentially transmitted organisms.

Our findings have important implications for hospital management and infection prevention. 55/149 patients (37%) in our study experienced BSIs, which is comparable to the rate of BSI in other transplant centers⁸⁴. Our findings suggest that microbiome transmission does not play a large role in spreading infections among HCT patients, and that established contact precautions and procedures for patient isolation were working as intended. Recently, the HCT ward at our hospital moved to a new location with exclusively single rooms, which may further reduce the opportunity for transmission.

Our analysis of transmission of microbes between HCT patients does have several limitations. We analyzed hundreds of samples collected over many years, but most sampling was done on a weekly basis. We did not explicitly collect samples on the day of admission or discharge. Our sample collection

also ignores previous hospital stays, either in a different ward in our hospital, or other hospitals entirely, that may be responsible for the acquisition of HAI organisms. We also did not perform any sampling of the hospital environment, healthcare workers or visitors. Our work is also entirely based on metagenomic sequencing data, which has its own challenges and sources of bias, including “barcode swapping”⁶⁸, which could contribute to false positive transmission findings. We measured the impact of barcode swapping in linked-read data, and eliminated linked-read and short-read comparisons where a finding of identical strains could be the result of barcode swapping (see supplemental note). While our comparison methods were sensitive to strain populations in the gut microbiome, we did not attempt to phase strain haplotypes. Haplotype phasing with long-read sequencing technology like Nanopore or PacBio^{85–87} could help us determine whether sets of SNPs occurred in the same or different strains.

Our study leaves several questions unanswered that we hope future work on microbiome transmission will attempt to answer. First, our findings need to be validated in an external cohort in a different hospital. Collecting stool samples during an infection outbreak may lead to more transmission events being identified and may implicate microbiome transmission in perpetuating the outbreak. Similar experiments in a pediatric patient population may reveal more gut-to-gut transmission, as young children have microbiomes that are still developing and more susceptible to colonization with new species. As more transmission events are observed with high-resolution genomic methods, we will start to uncover the general principles governing community assembly in the human microbiome. These new insights may help prevent infections and other co-morbidities in this patient population in the future.

Methods

Cohort selection

Hematopoietic cell transplantation patients were recruited at the Stanford Hospital Blood and Marrow Transplant Unit under an IRB-approved protocol (Protocol #8903; Principal Investigator: Dr. David Miklos, co-Investigator: Drs. Ami Bhatt and Tessa Andermann). Informed consent was obtained from all individuals whose samples were collected. Stool samples were placed at 4 °C immediately upon collection and processed for storage at the same or following day. Stool samples were aliquoted into 2-mL cryovial tubes and homogenized by brief vortexing. The aliquots were stored at -80 °C until extraction.

We identified all samples that had been sequenced previously by our group. Samples were selected for linked-read sequencing to augment this collection. We examined the network of patient roommate overlaps to find cases where we were likely to uncover transmission events, if they were happening. These included patient pairs from whom we ideally had samples before and after the roommate overlap period. 96 samples that provided the best coverage of roommate overlaps were selected for linked-read sequencing.

The following clinical data were extracted from the electronic health record: demographic information, underlying disease, type of transplantation (allogeneic vs. autologous), date and type of bloodstream infection, time of admission and discharge and location of patients (rooms) over time. Hospital-wide BSI data were obtained from an electronic report generated by the clinical microbiology laboratory.

DNA Extraction, library preparation and sequencing

DNA was extracted from stool samples using a mechanical bead-beating approach with the Mini-Beadbeater-16 (BioSpec Products) and 1-mm diameter zirconia/silica beads (BioSpec Products) followed by the QIAamp Fast DNA Stool Mini Kit (Qiagen) according to manufacturer's instructions. Bead-beating consisted of 7 rounds of alternating 30 s bead-beating bursts followed by 30 s of cooling on ice. For samples subjected to linked-read sequencing, DNA fragments less than approximately 2 kb

were eliminated with a SPRI bead purification approach⁸⁸ using a custom buffer with minor modifications: beads were added at 0.9×, and eluted DNA was resuspended in 50 µl of water. DNA concentration was quantified using a Qubit fluorometer (Thermo Fisher Scientific). DNA fragment length distributions were quantified using a TapeStation 4200 (Agilent Technologies).

Short-read sequencing libraries were prepared with either the Nextera Flex or Nextera XT kit (Illumina) according to manufacturer's instructions. Linked-read sequencing libraries were prepared on the 10X Genomics Chromium platform (10X Genomics). Linked-read libraries have a single sample index, and were pooled to minimize the possibility of barcode swapping between samples from patients who were roommates (see supplemental note). Libraries were sequenced on an Illumina HiSeq 4000 (Illumina).

Sequence data processing

TrimGalore version 0.5.0⁸⁹ was used to perform quality and adapter trimming with the flags “–clip_R1 15–clip_R2 15–length 60”. SeqKit version 0.9.1⁹⁰ was used to remove duplicates in short-read data with the command “seqkit rmdup–by-seq”. Due to excessive processing time, this step was skipped for linked-read data. Reads were mapped against the GRCh38 assembly of the human genome using BWA version 0.7.17-r1188⁹¹ and only unmapped reads were retained. Quality metrics were verified with FastQC version 0.11.8⁹². Bioinformatics workflows were implemented with Snakemake⁹³.

Short-read classification with Kraken2

We classified all short-read data with a Kraken2³⁹ database containing all bacteria, viral and fungal genomes in NCBI GenBank assembled to complete genome, chromosome or scaffold quality as of January 2020. Human and mouse reference genomes were also included in the database. A Bracken⁴⁰ database was also built with a read length of 150 and k-mer length of 35. Classification results were processed into matrices and taxonomic barplots with the workflow available at https://github.com/bhattlab/kraken2_classification.

Assembly and binning

Short-read sequencing samples were assembled using SPAdes version 3.14.0³⁰ using the ‘--meta’ flag. Linked-read sequencing samples were assembled with Megahit version 1.2.9³¹ to generate seed contigs, which were then assembled with the barcode-aware assembler Athena²⁶. Metagenome-assembled genomes (MAGs) were binned with Metabat2 version 2.15³², Maxbin version 2.2.7³³ and CONCOCT version 1.1.0³⁴ and aggregated using DASTool version 1.1.1³⁵. MAG completeness and contamination was evaluated using CheckM version 1.0.13³⁶ and MAG quality was evaluated by the standards set in³⁷. All assembled contigs were classified with Kraken2 as described above. To generate bin identifications, contig classifications were pooled such that contigs making up at least two thirds the length of the bin were classified as a particular species. If a classification could not be assigned at the species level, the process was repeated at the genus level, and so on.

Genome de-replication and SNP profiling

MAGs were filtered to have minimum completeness 50% and maximum contamination 15% as measured by CheckM, then were de-replicated with dRep version 2.6.2⁴⁸ with default parameters except the primary clustering threshold set to 0.95. In further steps, a single de-replicated genome will be referred to as a cluster. Reads from all samples were mapped against the de-replicated set of genomes with BWA. Clusters that had greater than 1x average coverage in at least two samples were retained for further analysis. Individual bam files were extracted for each sample-cluster pair with at least 1x coverage. Bam files were randomly subsetted to a maximum of 2 million reads for computational efficiency. Alignments were profiled and then compared across samples with inStrain version 1.3.11⁶⁶ using default parameters. A Snakemake workflow for dRep and inStrain analysis is available at https://github.com/bhattlab/bhattlab_workflows.

Building phylogenetic trees

MAG Average Nucleotide Identity (ANI) trees (Figure 2 and 3) were created using the pairwise alignment values from dRep, which uses the MUMmer program⁹⁴. MAGs were filtered to be at least 75% the length of the mean length of reference genomes used in the tree. Reference genomes were selected

by searching literature for collections of well-described isolates with genomes available. References that were not relevant and clustered in isolated sections of the tree were removed. Pairwise ANI values were transformed into a distance matrix and clustered using the 'hclust' function with the 'average' method in R version 4.0.3⁹⁵. Heatmaps were created using pairwise popANI values from inStrain, transformed into a distance matrix, and hierarchically clustered using the 'ward.D2' method.

Determining transmission thresholds

To determine the ANI threshold to call a comparison a “putative transmission event” we evaluated the distributions of ANI values for within- and between-patient comparisons for different species (Figure S3). We often detected zero population SNPs in time course samples from the same patient, including *E. faecium* in a pair of samples collected from the same patient 323 days apart. Meanwhile, between-patient comparisons typically had lower ANI values. To verify that transmission events would also result in population ANI values near 100%, we examined external datasets where transmission of bacteria in the microbiome is known to occur as a “positive control”. We gathered sequencing data from stool samples of matched mother-infant pairs¹⁸ and fecal microbiota transplantation donors and recipients⁶⁷ and processed them with the same methods. In these datasets, we regularly observed genomes with 100% popANI between matched individuals, and did not find cases of 100% popANI between unmatched individuals (Figure S4). In the ideal cases, we expect transmission of bacteria between the microbiomes of HCT patients to result in genomes with 100% popANI. However, the measured genomes may not reach this level of identity, due to mutations or genetic drift since the transmission event, sequencing errors, or other factors. Therefore, we set the transmission threshold at 99.999% popANI, equivalent to 30 population SNPs in a 3 megabase (Mb) genome. Although this threshold is stringent, we recognize that it may allow for false positives where two closely related strains exist in different patients solely by chance.

Pairwise MAG comparison

MAGs were aligned with the mummer program using default settings⁹⁴ and filtered for 1-1 alignments. Dotplots were visualized with the “Dot” program⁹⁶ filtering for non-repetitive alignments ≥ 1 kb.

Antibiotic resistance gene detection

Antibiotic resistance genes (ARGs) were profiled in contigs from all samples using Resistance Gene Identifier (RGI) and the Comprehensive Antibiotic Resistance Database (CARD)⁹⁷ with default parameters. Genes were counted if they met the “strict” or “perfect” threshold from RGI. ARGs were annotated both if they occurred on a contig in the MAG of interest, or anywhere in the metagenomic assembly.

Acknowledgements

We would like to acknowledge the contributions of several members of the Bhatt lab for their assistance in the experimental design, laboratory work and manuscript preparation, including C. Severyn, D. Maghini, S. Vance, A. Natarajan, P. West, A. Behr, M. Chakraborty and S. Zliniti. We would also like to thank B. Wu at Stanford Health Care for providing information on the geographic layout of the HCT ward, K. Chen for providing information relevant to restrictions on patients consuming probiotics, A. Sidow and Z. Weng for their instruction and assistance in preparing linked-read sequencing libraries and K. Siranosian for edits to the manuscript. This work was supported by NIH P01 CA049605 (PI: R. Negrin; Cell Therapy for Leukemia and Lymphoma), and NIH R01 AI143757, CDC BAA 75D30118C02921, and a Damon Runyon Clinical Investigator Award to A.S.B. B.A.S. is supported by a NIST JIMB training grant. Computing costs were supported via a NIH S10 Shared Instrumentation Grant 1S10OD02014101. This work utilized computing resources provided by the Stanford Genetics Bioinformatics Service Center. Finally, we would like to acknowledge the patients and nurses on the Blood and Marrow Transplantation service for their enthusiastic participation in this project.

Author Contributions

B.A.S., A.S.B., H.T., N.B., T.A. designed the study. B.A.S. performed laboratory and computational work, conducted the analysis and wrote the manuscript. E.B. performed laboratory work and contributed to writing the manuscript. T.A. performed laboratory work. A.R.R. and T.A. Designed the stool sample collection effort. N.B. assisted with analysis of BSI data. H.T. assisted with computational analysis. A.S.B. oversaw the project and contributed to writing of the manuscript. All authors contributed to editing the manuscript.

Competing Interests statement

The authors have no competing interests to declare.

Data availability

Raw sequence data for this manuscript, when not previously published, have been uploaded to NCBI SRA under project number PRJNA707487, which will be released under publication. MAGs generated in this study are available in a tar.gz archive (8.4 Gb) from Google Cloud Platform:

https://storage.googleapis.com/gpsc-gcp-lab-bhatt_public/transmission/MAGs.tar.gz. Workflows for data processing, Kraken2 Classification, MAG binning and inStrain comparisons can be found at https://github.com/bhattlab/bhattlab_workflows. Days of roommate and hospital overlap between patients is provided in Tables S9 and S10.

Table titles

1. Aggregated characteristics of patients with samples investigated in this study.
2. Aggregated statistics of temporal geographic data for all patients on the ward during the study period.
3. Aggregated statistics of sequencing datasets and metagenome-assembled genomes (MAGs) generated in this study.

Supplemental table titles

1. Clinical metadata of patients with samples investigated in this study.
2. Sequencing datasets analyzed in this study.
3. Statistics on MAGs generated in this study.
4. Kraken2 classification results for all samples at the species level. Species with less than 0.01% abundance have been removed.
5. Kraken2 classification results for all samples at the genus level. Genera with less than 0.01% abundance have been removed.
6. Source and publication for each reference genome used in Figures 2 and 3.

7. Pairwise alignment-based ANI for *Escherichia coli* and *Enterococcus faecium* genomes analyzed in Figures 2 and 3. MAGs are identified by a concatenation of the seq_id and Bin columns in Table S3.
8. InStrain results for all comparisons made between samples in this manuscript. Filtered to remove comparisons <99.99% popANI, <0.5 percent_compared and potential barcode swapping results.
9. Matrix of number of days patients overlapped in the hospital.
10. Matrix of number of days patients overlapped as roommates.

Supplemental note: Mitigation of laboratory contamination and barcode swapping

Any study of transmission is susceptible to confounders that may introduce false positives. Two major sources are laboratory contamination and barcode swapping, both of which can make it appear as if identical strains were present in multiple samples. To minimize the chance of laboratory contamination, samples selected for linked-read sequencing were randomized prior to extraction into groups of 16, subject to the constraint that the number of samples from roommate pairs in the same extraction batch were minimized. These groupings were carried out through library preparation. Similar constraints were used when preparing pooled libraries for sequencing.

It is a recognized phenomenon that pooled Illumina sequencing libraries experience “barcode swapping” or “index hopping”⁶⁸ when libraries are differentiated by a single sample index. While this issue is avoided by using unique dual index sequences for all samples in a pool, our laboratory was not aware of the issue until 2018, and older libraries were prepared without a unique dual indexing strategy. Linked-read libraries only contain a single sample index sequence, which makes it impossible to eliminate the effect of barcode swapping, other than the costly option of devoting an entire lane to each sample.

In linked-read sequencing libraries, we were able to estimate the impact of barcode swapping. There are ~10 million possible 10X barcodes (these are the barcodes which convey long-range information, different from the sample index barcodes). While a subset of 10X barcodes will overlap between two samples, the fraction of barcodes from reads mapping to a single organism should be limited. We mapped reads from all linked-read samples against the uniquely identifiable p-crAssphage genome⁹⁸. Then we looked at the fraction of 10X barcodes that overlapped between samples. Samples sequenced on different lanes typically had 0-30% 10X barcode overlap. Samples sequenced on the same lane had 60-100% of barcode overlap in some cases. We set a threshold of 40% overlap of barcode sets to call a comparison “swapped” and remove it from analysis. By counting reads believed to

be assigned to improper samples because of barcode swapping, we estimate the rate in our linked-read data to be 0.1-0.2%.

While this rate may seem small, at high sequencing depth and with abundant organisms, it quickly results in enough reads being swapped to assemble a genome or conduct an inStrain comparison. Indeed, we found cases where multiple species (instead of the single species believed to be the result of transmission events) were shared between linked-read samples sequenced on the same lane that were likely the result of barcode swapping.

For short-read sequencing samples, we know which pairs of samples share one of two index sequences and have the possibility of being impacted by swapping. We cannot estimate the impact of barcode swapping like was done for linked-read datasets. We simply eliminated all comparisons where two samples had the possibility of barcode swapping, and all comparisons that could be affected by “secondary” swapping, where the samples were not directly affected, but an interaction between other samples from the two patients could cause false positives. While this filtering may discard legitimate transmission events, we believe it is necessary to lower the number of false positives.

Previous DNA extraction and short-read sequencing efforts did not follow the randomization constraints above and we cannot guarantee that laboratory contamination did not happen at some point in the process. However, we note that cases of laboratory contamination or barcode swapping would result in the entire microbiome composition of one sample being transferred to another. After our stringent filters, we only discovered one case where patients shared two separate species. As these were both *Lactobacillus* species, our hypothesis about probiotic consumption is a possible explanation.

References

1. Young, J.-A. H. *et al.* Infections after Transplantation of Bone Marrow or Peripheral Blood Stem Cells from Unrelated Donors. *Biol. Blood Marrow Transplant.* 22, 359–370 (2016).
2. See, I. *et al.* Mucosal Barrier Injury Laboratory-Confirmed Bloodstream Infection: Results from a Field Test of a New National Healthcare Safety Network Definition. *Infect. Control Hosp. Epidemiol.* 34, 769–776 (2013).
3. Kelly, M. S. *et al.* Gut Colonization Preceding Mucosal Barrier Injury Bloodstream Infection in Pediatric Hematopoietic Stem Cell Transplantation Recipients. *Biol. Blood Marrow Transplant.* 25, 2274–2280 (2019).
4. Tamburini, F. B. *et al.* Precision identification of diverse bloodstream pathogens in the gut microbiome. *Nat. Med.* 1 (2018) doi:10.1038/s41591-018-0202-8.
5. Zhai, B. *et al.* High-resolution mycobiota analysis reveals dynamic intestinal translocation preceding invasive candidiasis. *Nat. Med.* 1–6 (2020) doi:10.1038/s41591-019-0709-7.
6. Taur, Y. *et al.* Intestinal Domination and the Risk of Bacteremia in Patients Undergoing Allogeneic Hematopoietic Stem Cell Transplantation. *Clin. Infect. Dis.* 55, 905–914 (2012).
7. Ubeda, C. *et al.* Vancomycin-resistant *Enterococcus* domination of intestinal microbiota is enabled by antibiotic treatment in mice and precedes bloodstream invasion in humans. *J. Clin. Invest.* 120, 4332–4341 (2010).
8. Jenq, R. R. *et al.* Intestinal *Blautia* Is Associated with Reduced Death from Graft-versus-Host Disease. *Biol. Blood Marrow Transplant.* 21, 1373–1383 (2015).
9. Mathewson, N. D. *et al.* Gut microbiome–derived metabolites modulate intestinal epithelial cell damage and mitigate graft-versus-host disease. *Nat. Immunol.* 17, 505–513 (2016).
10. Peled, J. U. *et al.* Microbiota as Predictor of Mortality in Allogeneic Hematopoietic-Cell Transplantation. *N. Engl. J. Med.* 382, 822–834 (2020).

11. Shono, Y. *et al.* Increased GVHD-related mortality with broad-spectrum antibiotic use after allogeneic hematopoietic stem cell transplantation in human patients and mice. *Sci. Transl. Med.* 8, 339ra71 (2016).
12. Taur, Y. *et al.* The effects of intestinal tract bacterial diversity on mortality following allogeneic hematopoietic stem cell transplantation. *Blood* 124, 1174–1182 (2014).
13. Weber, D. *et al.* Microbiota Disruption Induced by Early Use of Broad-Spectrum Antibiotics Is an Independent Risk Factor of Outcome after Allogeneic Stem Cell Transplantation. *Biol. Blood Marrow Transplant.* 23, 845–852 (2017).
14. L. Livornese Jr, L. *et al.* Hospital-acquired Infection with Vancomycin-resistant *Enterococcus faecium* Transmitted by Electronic Thermometers. *Ann. Intern. Med.* (1992).
15. Raven, K. E. *et al.* Complex Routes of Nosocomial Vancomycin-Resistant *Enterococcus faecium* Transmission Revealed by Genome Sequencing. *Clin. Infect. Dis.* 64, 886–893 (2017).
16. Bäckhed, F. *et al.* Dynamics and Stabilization of the Human Gut Microbiome during the First Year of Life. *Cell Host Microbe* 17, 690–703 (2015).
17. Siranosian, B. A., Tamburini, F. B., Sherlock, G. & Bhatt, A. S. Acquisition, transmission and strain diversity of human gut-colonizing crAss-like phages. *Nat. Commun.* 11, 1–11 (2020).
18. Yassour, M. *et al.* Strain-Level Analysis of Mother-to-Child Bacterial Transmission during the First Few Months of Life. *Cell Host Microbe* 24, 146-154.e4 (2018).
19. Lozupone, C. A., Stombaugh, J. I., Gordon, J. I., Jansson, J. K. & Knight, R. Diversity, stability and resilience of the human gut microbiota. *Nature* 489, 220–230 (2012).
20. Suez, J. *et al.* Post-Antibiotic Gut Mucosal Microbiome Reconstitution Is Impaired by Probiotics and Improved by Autologous FMT. *Cell* 174, 1406-1423.e16 (2018).
21. Zmora, N. *et al.* Personalized Gut Mucosal Colonization Resistance to Empiric Probiotics Is Associated with Unique Host and Microbiome Features. *Cell* 174, 1388-1405.e21 (2018).
22. Brito, I. L. *et al.* Transmission of human-associated microbiota along family and social networks. *Nat. Microbiol.* 1 (2019) doi:10.1038/s41564-019-0409-6.

23. Andermann, T. M. *et al.* The Microbiome and Hematopoietic Cell Transplantation: Past, Present, and Future. *Biol. Blood Marrow Transplant.* 24, 1322–1340 (2018).
24. Rashidi, A. *et al.* Pre-transplant recovery of microbiome diversity without recovery of the original microbiome. *Bone Marrow Transplant.* 1 (2018) doi:10.1038/s41409-018-0414-z.
25. Shono, Y. & van den Brink, M. R. M. Gut microbiota injury in allogeneic haematopoietic stem cell transplantation. *Nat. Rev. Cancer* 18, 283–295 (2018).
26. Bishara, A. *et al.* High-quality genome sequences of uncultured microbes by assembly of read clouds. *Nat. Biotechnol.* (2018) doi:10.1038/nbt.4266.
27. Kang, J. B. *et al.* Intestinal microbiota domination under extreme selective pressures characterized by metagenomic read cloud sequencing and assembly. *BMC Bioinformatics* 20, 585 (2019).
28. Truong, D. T., Tett, A., Pasolli, E., Huttenhower, C. & Segata, N. Microbial strain-level population structure and genetic diversity from metagenomes. *Genome Res.* 27, 626–638 (2017).
29. Van Rossum, T., Ferretti, P., Maistrenko, O. M. & Bork, P. Diversity within species: interpreting strains in microbiomes. *Nat. Rev. Microbiol.* 1–16 (2020) doi:10.1038/s41579-020-0368-1.
30. Nurk, S., Meleshko, D., Korobeynikov, A. & Pevzner, P. A. metaSPAdes: a new versatile metagenomic assembler. *Genome Res.* 27, 824–834 (2017).
31. Li, D., Liu, C.-M., Luo, R., Sadakane, K. & Lam, T.-W. MEGAHIT: an ultra-fast single-node solution for large and complex metagenomics assembly via succinct de Bruijn graph. *Bioinforma. Oxf. Engl.* 31, 1674–1676 (2015).
32. Kang, D. D. *et al.* MetaBAT 2: an adaptive binning algorithm for robust and efficient genome reconstruction from metagenome assemblies. *PeerJ* 7, e7359 (2019).
33. Wu, Y.-W., Simmons, B. A. & Singer, S. W. MaxBin 2.0: an automated binning algorithm to recover genomes from multiple metagenomic datasets. *Bioinformatics* 32, 605–607 (2016).
34. Alneberg, J. *et al.* Binning metagenomic contigs by coverage and composition. *Nat. Methods* 11, 1144–1146 (2014).

35. Sieber, C. M. K. *et al.* Recovery of genomes from metagenomes via a dereplication, aggregation and scoring strategy. *Nat. Microbiol.* 1 (2018) doi:10.1038/s41564-018-0171-1.
36. Parks, D. H., Imelfort, M., Skennerton, C. T., Hugenholtz, P. & Tyson, G. W. CheckM: assessing the quality of microbial genomes recovered from isolates, single cells, and metagenomes. *Genome Res.* gr.186072.114 (2015) doi:10.1101/gr.186072.114.
37. Bowers, R. M. *et al.* Minimum information about a single amplified genome (MISAG) and a metagenome-assembled genome (MIMAG) of bacteria and archaea. *Nat. Biotechnol.* 35, 725–731 (2017).
38. Almeida, A. *et al.* A unified catalog of 204,938 reference genomes from the human gut microbiome. *Nat. Biotechnol.* 1–10 (2020) doi:10.1038/s41587-020-0603-3.
39. Wood, D. E., Lu, J. & Langmead, B. Improved metagenomic analysis with Kraken 2. *Genome Biol.* 20, 1–13 (2019).
40. Lu, J., Breitwieser, F. P., Thielen, P. & Salzberg, S. L. Bracken: estimating species abundance in metagenomics data. *PeerJ Comput. Sci.* 3, e104 (2017).
41. Centers for Disease Control and Prevention (U.S.). Diseases and Organisms in Healthcare Settings | HAI | CDC. <https://www.cdc.gov/hai/organisms/organisms.html> (2019).
42. Lloyd-Price, J. *et al.* Strains, functions and dynamics in the expanded Human Microbiome Project. *Nature* 550, 61–66 (2017).
43. Abranches, J. *et al.* Biology of Oral Streptococci. *Microbiol. Spectr.* 6, (2018).
44. Dubin, K. & Pamer, E. G. Enterococci and Their Interactions with the Intestinal Microbiome. *Bugs Drugs* 309–330 (2018) doi:10.1128/microbiolspec.BAD-0014-2016.
45. Palmer, K. L. *et al.* Comparative Genomics of Enterococci: Variation in *Enterococcus faecalis*, Clade Structure in *E. faecium*, and Defining Characteristics of *E. gallinarum* and *E. casseliflavus*. *mBio* 3, (2012).
46. Tenailon, O., Skurnik, D., Picard, B. & Denamur, E. The population genetics of commensal *Escherichia coli*. *Nat. Rev. Microbiol.* 8, 207–217 (2010).

47. Kittana, H. *et al.* Commensal *Escherichia coli* Strains Can Promote Intestinal Inflammation via Differential Interleukin-6 Production. *Front. Immunol.* 9, (2018).
48. Olm, M. R., Brown, C. T., Brooks, B. & Banfield, J. F. dRep: a tool for fast and accurate genomic comparisons that enables improved genome recovery from metagenomes through de-replication. *ISME J.* 11, 2864–2868 (2017).
49. Forde, B. M. *et al.* The Complete Genome Sequence of *Escherichia coli* EC958: A High Quality Reference Sequence for the Globally Disseminated Multidrug Resistant *E. coli* O25b:H4-ST131 Clone. *PLOS ONE* 9, e104400 (2014).
50. Andersen, P. S. *et al.* Complete Genome Sequence of the Epidemic and Highly Virulent CTX-M-15-Producing H30-Rx Subclone of *Escherichia coli* ST131. *Genome Announc.* 1, (2013).
51. Gurnee, E. A. *et al.* Gut Colonization of Healthy Children and Their Mothers With Pathogenic Ciprofloxacin-Resistant *Escherichia coli*. *J. Infect. Dis.* 212, 1862–1868 (2015).
52. Whitmer, G. R., Moorthy, G. & Arshad, M. The pandemic *Escherichia coli* sequence type 131 strain is acquired even in the absence of antibiotic exposure. *PLOS Pathog.* 15, e1008162 (2019).
53. Madigan, T. *et al.* Extensive Household Outbreak of Urinary Tract Infection and Intestinal Colonization due to Extended-Spectrum β -Lactamase–Producing *Escherichia coli* Sequence Type 131. *Clin. Infect. Dis.* 61, e5–e12 (2015).
54. Schaufler, K. *et al.* Genomic and Functional Analysis of Emerging Virulent and Multidrug-Resistant *Escherichia coli* Lineage Sequence Type 648. *Antimicrob. Agents Chemother.* 63, (2019).
55. Paulshus, E. *et al.* Repeated Isolation of Extended-Spectrum- β -Lactamase-Positive *Escherichia coli* Sequence Types 648 and 131 from Community Wastewater Indicates that Sewage Systems Are Important Sources of Emerging Clones of Antibiotic-Resistant Bacteria. *Antimicrob. Agents Chemother.* 63, (2019).
56. Müller, A., Stephan, R. & Nüesch-Inderbinnen, M. Distribution of virulence factors in ESBL-producing *Escherichia coli* isolated from the environment, livestock, food and humans. *Sci. Total Environ.* 541, 667–672 (2016).

57. Ewers, C. *et al.* CTX-M-15-D-ST648 Escherichia coli from companion animals and horses: another pandemic clone combining multiresistance and extraintestinal virulence? *J. Antimicrob. Chemother.* 69, 1224–1230 (2014).
58. Henderson, T. A., Young, K. D., Denome, S. A. & Elf, P. K. AmpC and AmpH, proteins related to the class C beta-lactamases, bind penicillin and contribute to the normal morphology of Escherichia coli. *J. Bacteriol.* 179, 6112–6121 (1997).
59. Tedim, A. P. *et al.* Complete Genome Sequences of Isolates of Enterococcus faecium Sequence Type 117, a Globally Disseminated Multidrug-Resistant Clone. *Genome Announc.* 5, (2017).
60. Ahmed, M. O. & Baptiste, K. E. Vancomycin-Resistant Enterococci: A Review of Antimicrobial Resistance Mechanisms and Perspectives of Human and Animal Health. *Microb. Drug Resist.* 24, 590–606 (2017).
61. Altschul, S. F., Gish, W., Miller, W., Myers, E. W. & Lipman, D. J. Basic local alignment search tool. *J. Mol. Biol.* 215, 403–410 (1990).
62. Byrne, M., Rouch, D. & Skurray, R. Nucleotide sequence analysis of IS256 from the Staphylococcus aureus gentamicin-tobramycin-kanamycin-resistance transposon Tn4001. *Gene* 81, 361–367 (1989).
63. Hennig, S. & Ziebuhr, W. Characterization of the Transposase Encoded by IS256, the Prototype of a Major Family of Bacterial Insertion Sequence Elements. *J. Bacteriol.* 192, 4153–4163 (2010).
64. Kleinert, F. *et al.* Influence of IS256 on Genome Variability and Formation of Small-Colony Variants in Staphylococcus aureus. *Antimicrob. Agents Chemother.* 61, (2017).
65. Pulido-Tamayo, S. *et al.* Frequency-based haplotype reconstruction from deep sequencing data of bacterial populations. *Nucleic Acids Res.* 43, e105–e105 (2015).
66. Olm, M. R. *et al.* inStrain profiles population microdiversity from metagenomic data and sensitively detects shared microbial strains. *Nat. Biotechnol.* (2021) doi:10.1038/s41587-020-00797-0.
67. Smillie, C. S. *et al.* Strain Tracking Reveals the Determinants of Bacterial Engraftment in the Human Gut Following Fecal Microbiota Transplantation. *Cell Host Microbe* 23, 229-240.e5 (2018).

68. Minimizing Index Hopping. <https://www.illumina.com/techniques/sequencing/ngs-library-prep/multiplexing/index-hopping.html>.
69. Schluter, J. *et al.* The gut microbiota is associated with immune cell dynamics in humans. *Nature* 588, 303–307 (2020).
70. D’Amico, F. *et al.* Gut resistome plasticity in pediatric patients undergoing hematopoietic stem cell transplantation. *Sci. Rep.* 9, 5649 (2019).
71. Simms-Waldrup, T. R. *et al.* Antibiotic-Induced Depletion of Anti-inflammatory Clostridia Is Associated with the Development of Graft-versus-Host Disease in Pediatric Stem Cell Transplantation Patients. *Biol. Blood Marrow Transplant.* 23, 820–829 (2017).
72. Olm, M. R. *et al.* Necrotizing enterocolitis is preceded by increased gut bacterial replication, *Klebsiella*, and fimbriae-encoding bacteria. *Sci. Adv.* 5, eaax5727 (2019).
73. Howden, B. P. *et al.* Genomic Insights to Control the Emergence of Vancomycin-Resistant Enterococci. *mBio* 4, (2013).
74. Browne, H. P. *et al.* Culturing of ‘unculturable’ human microbiota reveals novel taxa and extensive sporulation. *Nature* 533, 543–546 (2016).
75. Kaur, S., Yawar, M., Kumar, P. A. & Suresh, K. *Hungatella effluvii* gen. nov., sp. nov., an obligately anaerobic bacterium isolated from an effluent treatment plant, and reclassification of *Clostridium hathewayi* as *Hungatella hathewayi* gen. nov., comb. nov. *Int. J. Syst. Evol. Microbiol.* 64, 710–718 (2014).
76. Atarashi, K. *et al.* T reg induction by a rationally selected mixture of Clostridia strains from the human microbiota. *Nature* 500, 232–236 (2013).
77. Linscott, A. J. *et al.* Fatal septicemia due to *Clostridium hathewayi* and *Campylobacter hominis*. *Anaerobe* 11, 97–98 (2005).
78. Woo, P. C. Y. *et al.* Bacteremia Due to *Clostridium hathewayi* in a Patient with Acute Appendicitis. *J. Clin. Microbiol.* 42, 5947–5949 (2004).

79. Reunanen, J. *et al.* Akkermansia muciniphila Adheres to Enterocytes and Strengthens the Integrity of the Epithelial Cell Layer. *Appl Env. Microbiol* 81, 3655–3662 (2015).
80. Yi, S. H., Jernigan, J. A. & McDonald, L. C. Prevalence of probiotic use among inpatients: A descriptive study of 145 U.S. hospitals. *Am. J. Infect. Control* 44, 548–553 (2016).
81. Pittet, V., Ewen, E., Bushell, B. R. & Ziola, B. Genome Sequence of Lactobacillus rhamnosus ATCC 8530. *J. Bacteriol.* 194, 726–726 (2012).
82. Forster, S. C. *et al.* A human gut bacterial genome and culture collection for improved metagenomic analyses. *Nat. Biotechnol.* 37, 186–192 (2019).
83. Fukami, T. Historical Contingency in Community Assembly: Integrating Niches, Species Pools, and Priority Effects. *Annu. Rev. Ecol. Evol. Syst.* 46, 1–23 (2015).
84. Dandoy, C. E., Ardura, M. I., Papanicolaou, G. A. & Auletta, J. J. Bacterial bloodstream infections in the allogeneic hematopoietic cell transplant patient: new considerations for a persistent nemesis. *Bone Marrow Transplant.* 52, 1091–1106 (2017).
85. Bertrand, D. *et al.* Hybrid metagenomic assembly enables high-resolution analysis of resistance determinants and mobile elements in human microbiomes. *Nat. Biotechnol.* 1 (2019) doi:10.1038/s41587-019-0191-2.
86. Moss, E. L., Maghini, D. G. & Bhatt, A. S. Complete, closed bacterial genomes from microbiomes using nanopore sequencing. *Nat. Biotechnol.* 1–7 (2020) doi:10.1038/s41587-020-0422-6.
87. Tsai, Y.-C. *et al.* Resolving the Complexity of Human Skin Metagenomes Using Single-Molecule Sequencing. *mBio* 7, (2016).
88. Ramawatar. DNA size selection (>3-4kb) and purification of DNA using an improved homemade SPRI beads solution. (2018) doi:10.17504/protocols.io.n7hdhj6.
89. Babraham Bioinformatics - Trim Galore!
https://www.bioinformatics.babraham.ac.uk/projects/trim_galore/.
90. Shen, W., Le, S., Li, Y. & Hu, F. SeqKit: A Cross-Platform and Ultrafast Toolkit for FASTA/Q File Manipulation. *PLOS ONE* 11, e0163962 (2016).

91. Li, H. & Durbin, R. Fast and accurate short read alignment with Burrows–Wheeler transform. *Bioinformatics* (2009).
92. Babraham Bioinformatics - FastQC A Quality Control tool for High Throughput Sequence Data. <https://www.bioinformatics.babraham.ac.uk/projects/fastqc/>.
93. Köster, J. & Rahmann, S. Snakemake—a scalable bioinformatics workflow engine. *Bioinformatics* 28, 2520–2522 (2012).
94. Kurtz, S. *et al.* Versatile and open software for comparing large genomes. *Genome Biol.* 5, R12 (2004).
95. R Development Core Team. *R: A Language and Environment for Statistical Computing.* (2012).
96. Nattestad, M. *MariaNattestad/dot.* (2020).
97. Alcock, B. P. *et al.* CARD 2020: antibiotic resistome surveillance with the comprehensive antibiotic resistance database. *Nucleic Acids Res.* (2019) doi:10.1093/nar/gkz935.
98. Dutilh, B. E. *et al.* A highly abundant bacteriophage discovered in the unknown sequences of human faecal metagenomes. *Nat. Commun.* 5, 4498 (2014).

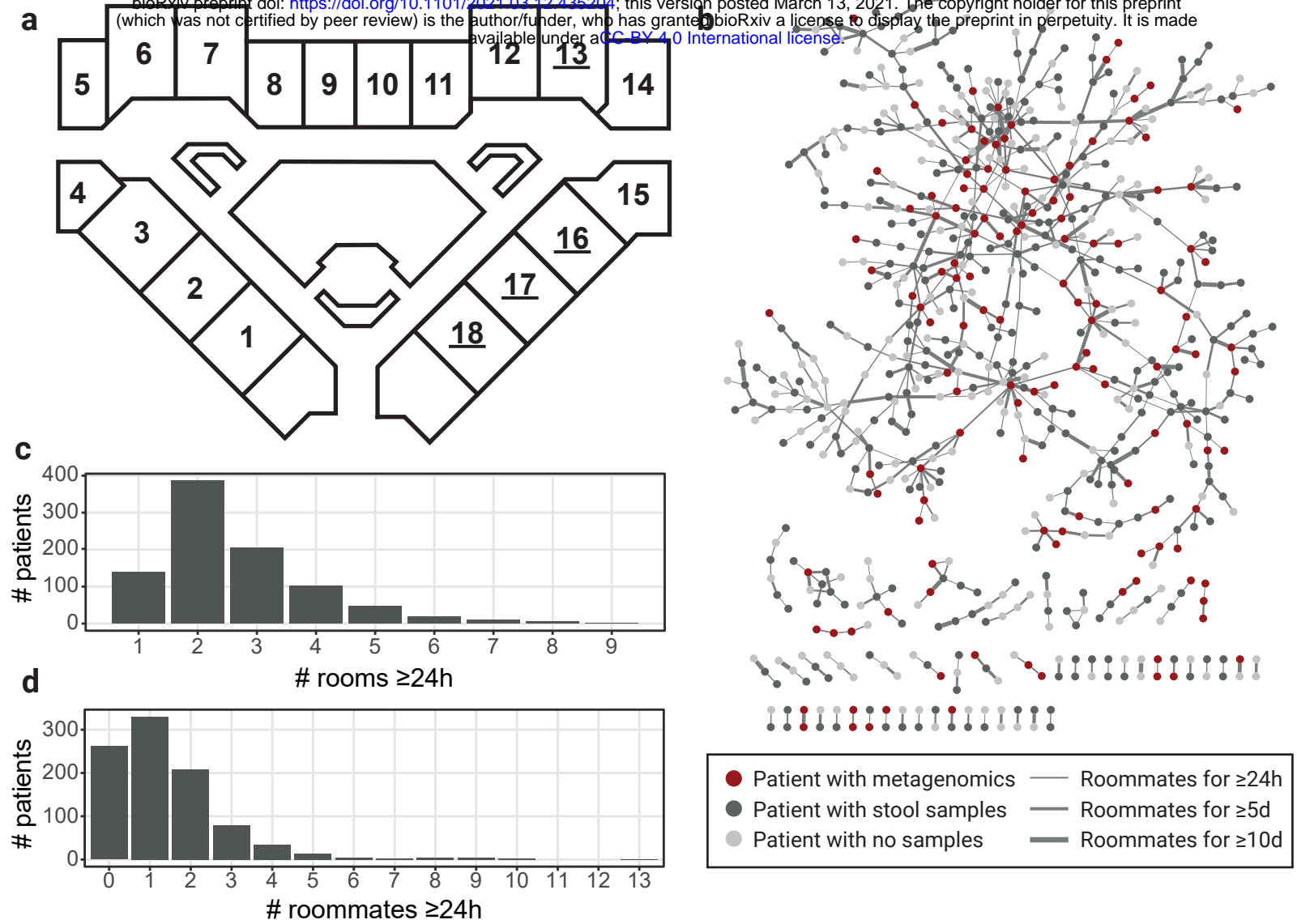


Figure S1: Analysis of hospital geography.

a) Layout of rooms in the HCT ward. Room numbers are indicated and double occupancy rooms are underlined.

b) Network view of patients who were roommates for at least 24 hours. Each node represents a single patient, colored according to if they have a banked stool sample or metagenomic sequencing data present. Edges are drawn between patients who were roommates, and edge width represents the length of overlap in the same room.

c) Histogram of the number of rooms patients occupied for at least 24 hours.

d) Histogram of the number of unique roommates patients had for at least 24 hours.

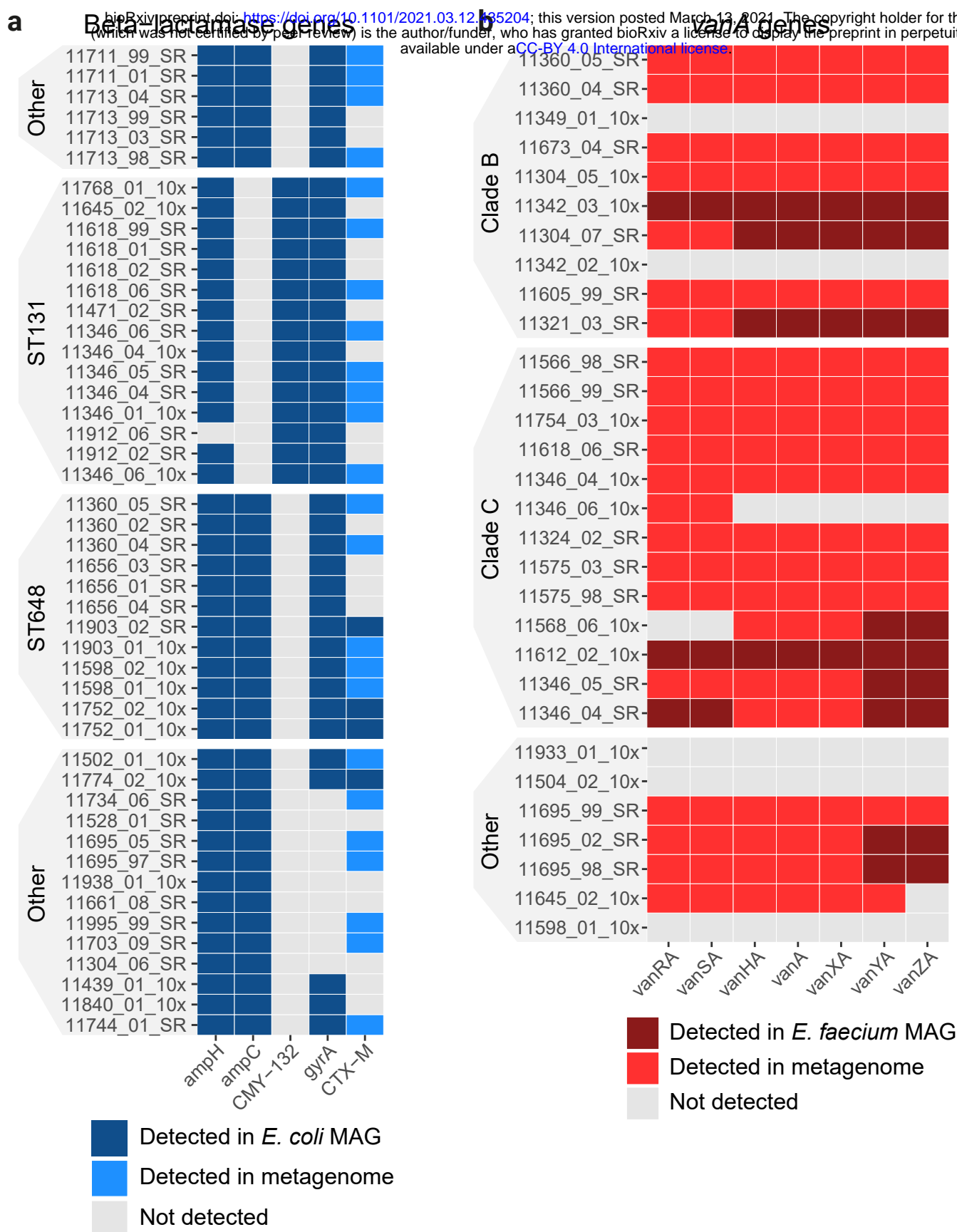


Figure S2: Antibiotic resistance genes detected. In each panel, samples are rows and resistance genes are columns. Samples are ordered and clades are highlighted corresponding to the respective figure in the main text. Cells are colored whether the gene was detected in the respective MAG from the sample, or just in the metagenome (indicating it may be on a plasmid).

a) Beta-lactamase genes detected in *E. coli* samples from Figure 2. The *gyrA* gene was detected with the CARD protein variant model, which requires a genetic variant conveying resistance in addition to the presence of the gene.

b) Vancomycin resistance genes of the *vanA* operon detected in *E. faecium* in samples from Figure 3.

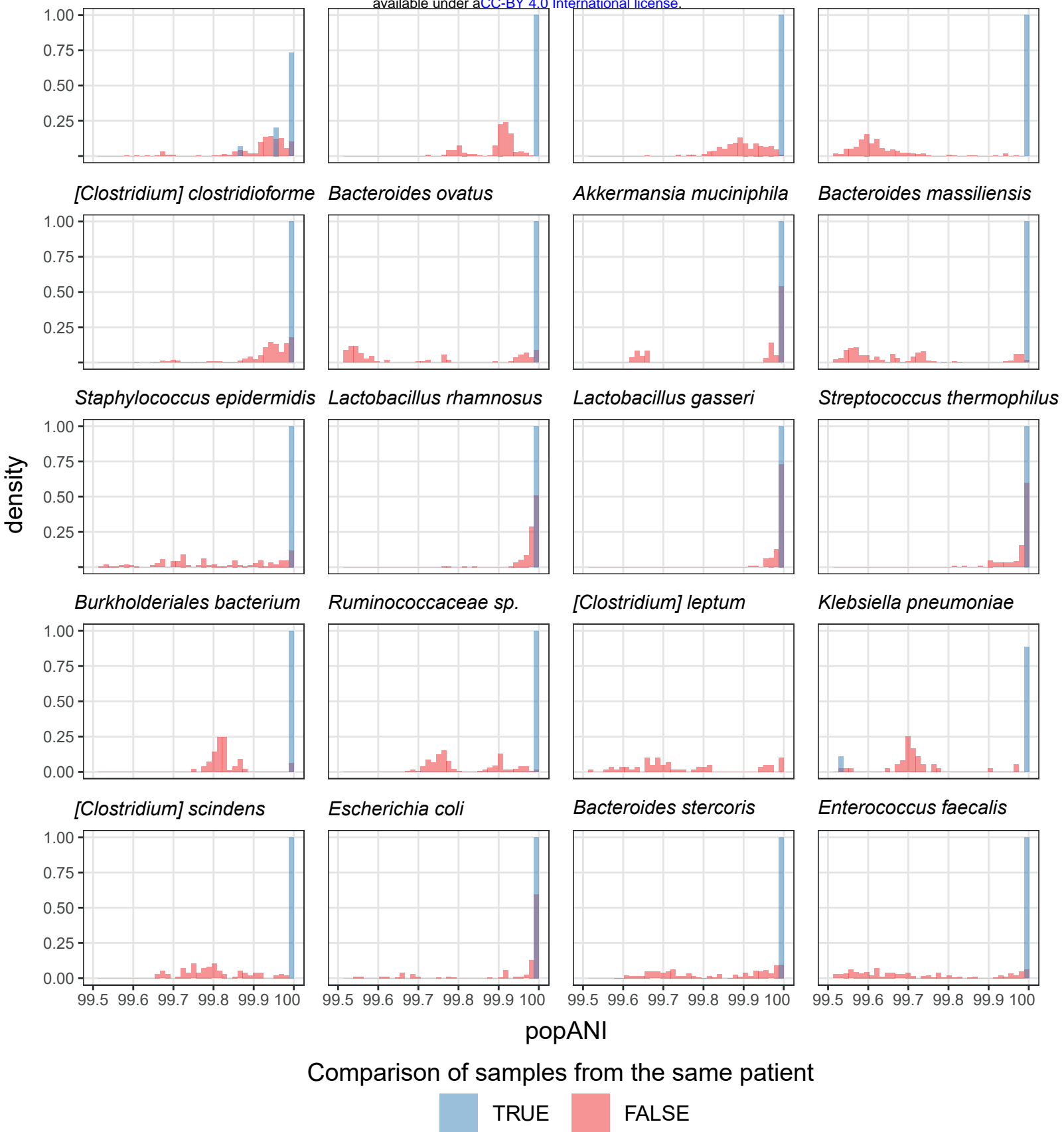
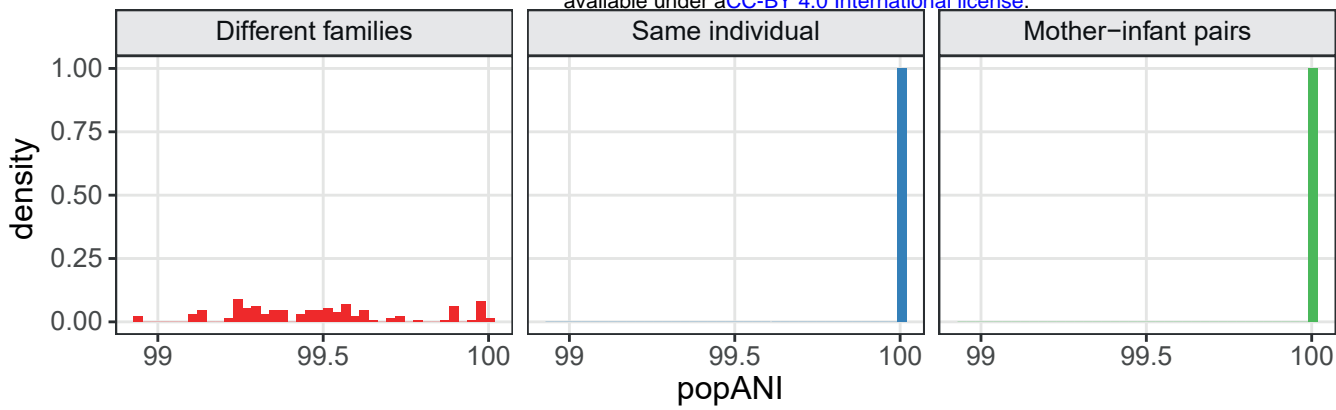


Figure S3: Distribution of popANI values comparing samples from the same or different patients. Distributions are split by species and the most common 25 species are shown. While in many cases the two distributions overlap, very rarely did popANI values comparing samples from different patients exceed the 99.999% transmission threshold. Comparisons with <99.5% popANI are omitted from the figure for clarity.

a

InStrain comparisons in Yassour et al. (2018)



b

InStrain comparisons in Smillie et al. (2018)

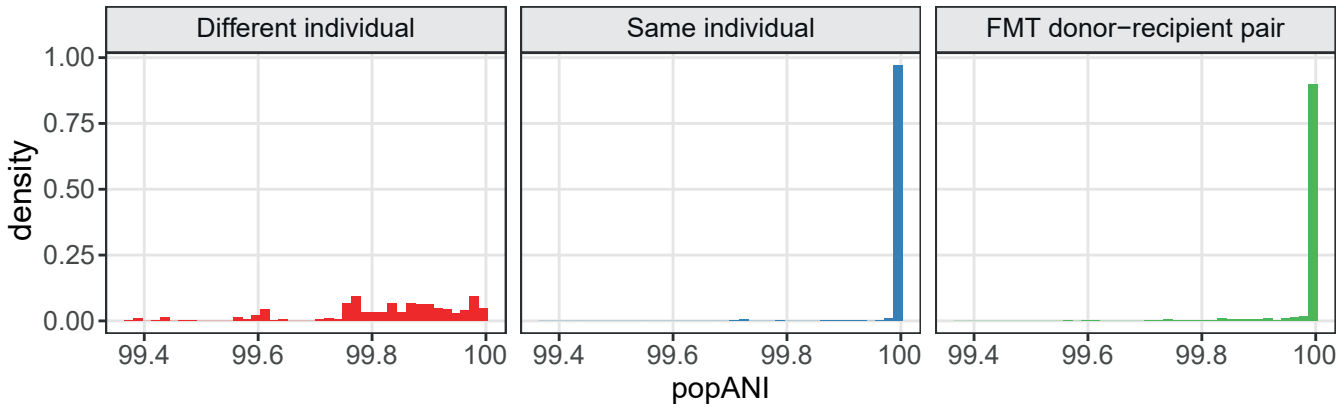


Figure S4: InStrain analysis of the five most common species in external datasets where transmission is expected to occur. Distributions of popANI values are separated based on the individuals the samples came from, with putative transmission events contained in the far right panel.

a) Metagenomic sequencing datasets from mother-infant pairs¹⁸. The maximum popANI value obtained when comparing samples from different families was 99.995%.

b) Metagenomic sequencing datasets from fecal microbiota transplantation donors and recipients⁶⁷. The maximum popANI value obtained comparing samples from individuals not related by FMT was 99.998%.

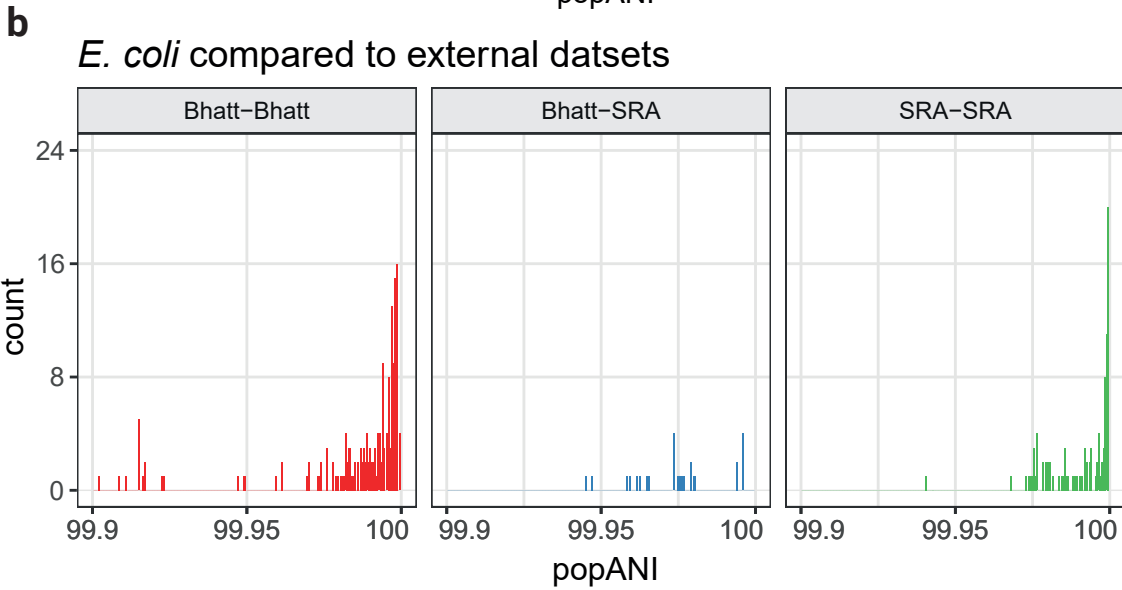
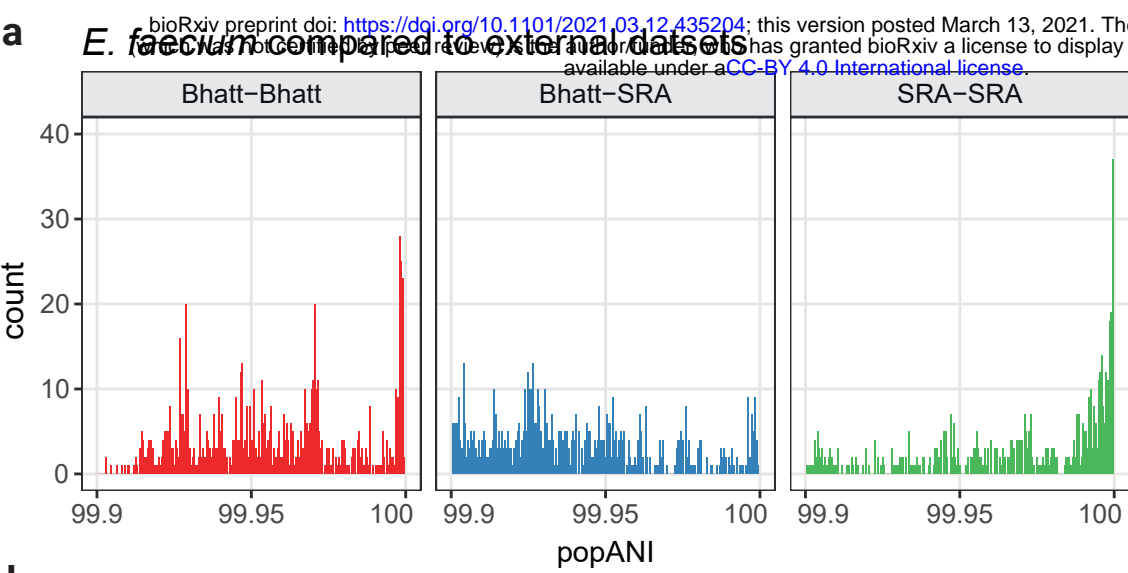


Figure S5: *Enterococcus faecium* (a) and *Escherichia coli* (b) strains compared to external datasets, including hospitalized adult and pediatric HCT patients, hospitalized infants and vancomycin-resistant *E. faecium* isolates^{3,69-73}. Panels are separated according to whether comparisons were made within the data in this manuscript (Bhatt-Bhatt), between our data and external data (Bhatt-SRA) or within external data (SRA-SRA).

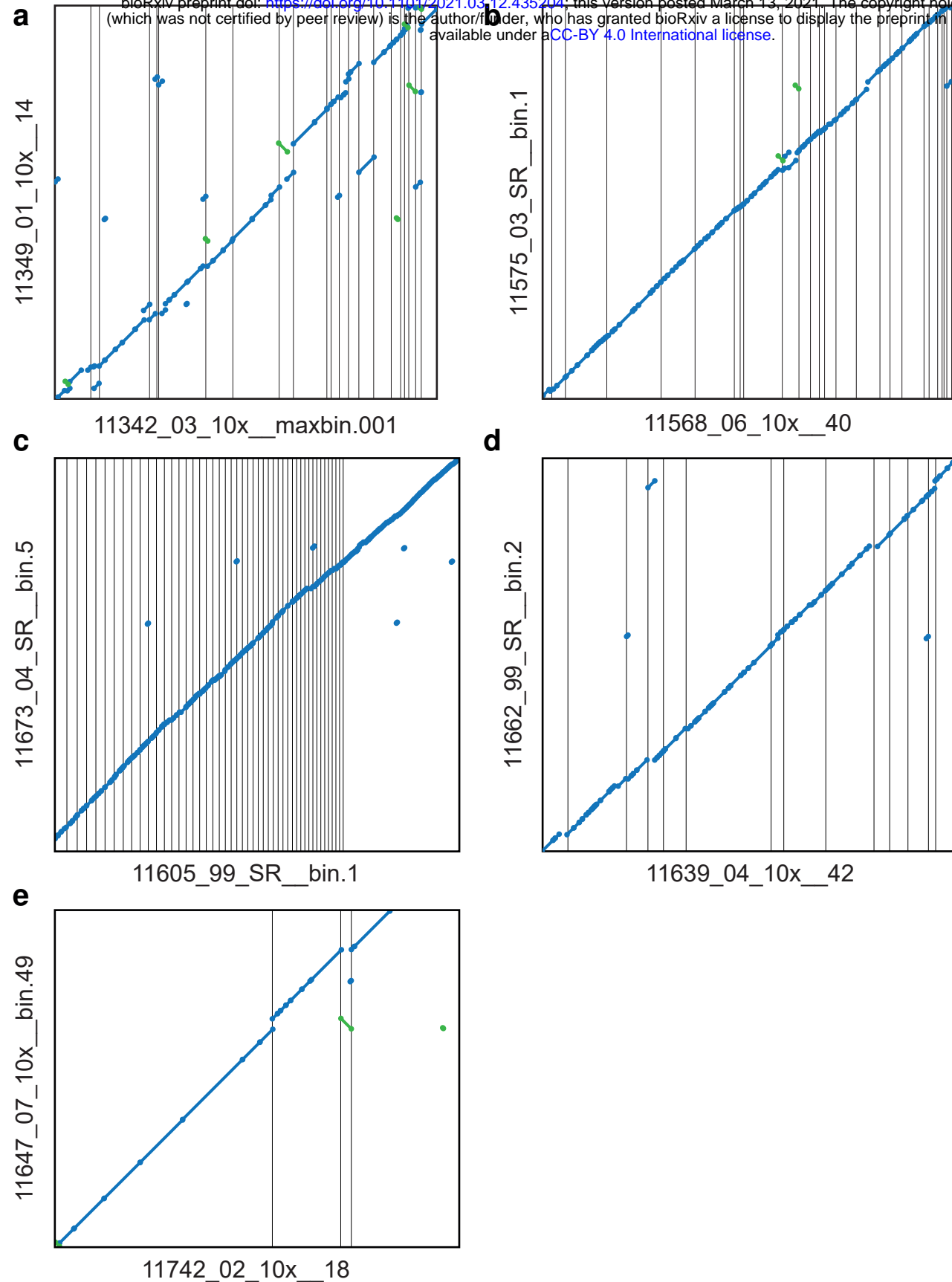


Figure S6: Dotplots showing pairwise alignment of MAGs in cases of putative transmission of the given species. Blue lines along the diagonal indicate 1-1 homology between the two sequences. Green lines indicate inversions that are likely the result of assembly or binning errors.

- a) *E. faecium* MAGs from patients 11342 and 11349, corresponding to figure 4a.
- b) *E. faecium* MAGs from patients 11575 and 11568, corresponding to figure 4b.
- c) *E. faecium* MAGs from patients 11605 and 11673, corresponding to figure 4c.
- d) *H. hathewayi* MAGs from patients 11639 and 11662, corresponding to figure 5a.
- e) *A. muciniphila* MAGs from patients 11742 and 11647 corresponding to figure 5b.

Table 1. Patient Characteristics

Attribute	n	%
Total sequenced patients	149	100%
AGE		
<=30	9	6%
31-40	17	11%
41-50	24	16%
51-60	38	26%
61-70	55	37%
>= 71	6	4%
SEX		
Sex M	87	58%
DIAGNOSIS		
ALL: Acute lymphocytic leukemia	21	14%
AML: Acute myelogenous leukemia	42	28%
CML: Chronic myeloid leukemia	6	4%
HL: Hodgkin lymphoma	4	3%
MDS: Myelodysplastic syndrome	42	28%
NHL: Non-Hodgkin lymphoma	23	15%
OTHER: Other malignancy	11	7%
GRAFT		
Allo	132	89%
Auto	17	11%
GVHD		
Accute GVHD yes	88	59%
Chronic GVHD yes	29	19%
Bloodstream Infection (BSI) Genera		
<i>Any BSI</i>	55	37%
Bacillus	1	1%
Enterobacter	3	2%
Enterococcus	7	5%
Escherichia	9	6%
Gemella	1	1%
Klebsiella	8	5%
Pseudomonas	2	1%
Rothia	4	3%
Staphylococcus	16	11%
Streptococcus	11	7%

Table 2. Roommate and Geographics

	all patients	patients with at least one sequenced sample
Number of patients spent ≥ 24h on ward	923	149
Days spent as inpatient on BMT ward		
Mean	21.9	37.6
Median	18	30.8
SD	18.2	21.8
Min	1	8.7
Max	175.4	137.7
Number of rooms occupied ≥ 24h		
Mean	2.6	3.5
Median	2	3
SD	1.3	1.7
Min	1	1
Max	9	9
Number of patients overlapped ≥ 24h		
Mean	55.9	80.8
Median	48	72
SD	30.7	38.6
Min	8	25
Max	246	198
Number of patients roommates ≥ 24h		
Mean	1.5	2.5
Median	1	2
SD	1.5	2.4
Min	0	0
Max	13	13

Table 3. Sequencing characteristics

Attribute	n		
Total stools sequenced	401		
Total sequencing datasets	405		
short read (SR)	312		
linked read (LR)	93		
Sequenced with SR and LR	4		
Samples sequenced per patient	median	range	SD
	2	1 - 13	2.4
Reads after processing (M)	median	range	SD
SR	7.6	0.01 - 28.8	4.4
LR	104	0.9 - 323.6	40
Assembly N50 (Kb)	median	range	SD
SR	17.2	0.7 - 163.6	24.8
LR	147.6	9.5 - 956.3	168.5
Binned genomes	n	%	
SR	2859		
High Quality	103	4%	
Medium Quality	2124	74%	
Low quality	632	22%	
LR	1900		
High Q Bowers	518	27%	
High Q Nayfach	950	50%	
Low quality	432	23%	